Research and Reports in Medicinal Chemistry

Dovepress
open access to scientific and medical research

Open Access Full Text Article

ORIGINAL RESEARCH

Pyrrolyl thiadiazoles as *Mycobacterium tuberculosis* inhibitors and their in silico analyses

This article was published in the following Dove Press journal:
Research and Reports in Medicinal Chemistry
28 April 2015
Number of times this article has been viewed

Shrinivas D Joshi[1]
Uttam A More[1,2]
Shailesh Sorathiya[1]
Deepshikha Koli[1]
Tejraj M Aminabhavi[1]

[1]Novel Drug Design and Discovery Laboratory, Department of Pharmaceutical Chemistry, Soniya Education Trust's College of Pharmacy, Dharwad, India; [2]Centre for Research and Development, Prist University, Thanjavur, Tamil Nadu, India

Abstract: A novel series of pyrrolyl thiadiazoles was synthesized and tested for antimycobacterial activity against the *Mycobacterium tuberculosis* $H_{37}Rv$ strain, using the microplate Alamar blue assay method. Molecular docking and in vitro minimum inhibitory concentration assays revealed that these molecules can be primarily screened for ENR inhibition, using the score values and H-bond interactions with amino acid residues Tyr158, Met98, and cofactor NAD^+, which are the key interactions. For most of the molecules, hydrophobic interaction is the key factor affecting their antitubercular activity. The activity of $-OCH_3$, $-NO_2$, -F, pyridine, and sulfonamide substituted derivatives was better than that of $-CH_3$, $-NH_2$, -Cl, and -Br substituted derivatives, as per experimental and docking studies. Molecular modeling studies are in agreement with their biological evaluations.

Keywords: pyrroles, antitubercular activity, Surflex-Docking, enoyl-ACP reductase

Introduction

Among the many infectious diseases, tuberculosis (TB) is one of the major ones caused by *Mycobacterium tuberculosis*.[1] Since 1993, the World Health Organization has identified TB as a global health emergency, with more than nine million new cases arising every year and an annual death toll of around 1.8 million people worldwide. The treatment of TB is a major problem, in view of the emergence of monodrug- and multidrug-resistant strains of *M. tuberculosis*.[2] Thus, there is an increasing need to develop novel anti-TB agents for the effective treatment of TB with reduced toxicity and enhanced activity against multidrug-resistance (MDR) strains for a short duration of therapy.

There are two discrete enzymes in the biosynthesis of fatty acids in bacteria; namely, fatty acid synthase (FAS) I and II. Type II fatty acid elongation system (FAS-II) of bacteria, in which reactions are catalyzed by different enzymes and each is encoded by a discrete gene, constitutes an attractive target for inhibition, as these enzymes differ significantly from type I FAS (FAS-I) in mammalians, in which enzymatic activities are encoded in one or two multifunctional polypeptides. *M. tuberculosis* possesses both FAS-I and FAS-II systems, of which FAS-I is responsible for bimodal distribution of products,[3,4] centered on C16 and C24–C26, but the FAS-II system prefers C16 as the starting substrate, which can extend[5] up to C56, indicating that mycobacterial FAS-II uses the products of FAS-I as the primers to extend fatty acyl chain lengths even further. The longer chain products of FAS-II are the precursors of mycolic acids, and both the systems provide precursors for biosynthesis of mycolic acids, which contain

Correspondence: Shrinivas D Joshi
Novel Drug Design and Discovery Laboratory, Department of Pharmaceutical Chemistry, Soniya Education Trust's College of Pharmacy, Sangolli Rayanna Nagar, Dharwad 580 002, India
Tel +91 998 615 1953
Fax +91 836 246 7190
Email shrinivasdj@rediffmail.com

very long chain fatty acids that are the prominent and essential components of the mycobacterial cell wall.[6,7]

The nicotinamide adenine dinucleotide-dependent enoyl-acyl carrier protein reductase encoded by *Mycobacterium* gene *inhA* has been validated as the primary molecular target of the frontline antitubercular drug, isoniazid.[8] Recent studies have demonstrated that InhA is also the target for the second-line antitubercular drug ethionamide.[9] As a prodrug, isoniazid must be activated by the mycobacterial catalase-peroxidase KatG into its acyl radical active form. However, some inhibitors can target InhA directly, without a requirement for activation similar to pyrazole derivatives, indole-5-amides,[10] alkyl diphenyl ethers,[11] and pyrrolidine carboxamides.[12] During our study, it was found that the InhA inhibitor, that is, 1-cyclohexyl-*N*-(3,5-dichlorophenyl)-5-oxopyrrolidine-3-carboxamide (pyrrolidine carboxamide or 641), contains three hydrophobic moieties, cyclohexyl, oxopyrrolidine, and 3,5-dichlorophenyl, which can be mapped by new designed molecules containing pyrrole, 1,3,4-thiadiazole, and substituted phenyl (see details in Figure S1). These findings prompted us to select InhA as the target for our newly designed molecules. Hence, by considering the nicotinamide adenine dinucleotide-dependent enoyl-acyl carrier protein reductase as the target receptor, we have performed molecular docking studies and screening for the supportive coordination between in silico studies and the in vitro results.

Pyrroles conform to an important class of heterocycles having a wide range of biological activities,[13] such as antitubercular, antiinflammatory, antiviral, and antiproliferative activities. The versatile and eminent biological profiles of 1,3,4-thiadiazoles and their analogs are well known.[14] Because of the presence of a toxophoric N=C-S moiety, 1,3,4-thiadiazoles exhibit a broad spectrum of biological activities. Recent literature suggests that 1,3,4-thiadiazole derivatives exhibit antibacterial and antitubercular activities.[15,16] On the basis these facts, and supported by the literature findings,[17–22] we propose synthesizing and testing the biological activities of a new type of pyrrolyl thiadiazole derivatives from 2-amino-5-substituted phenyl-1,3,4-thiadiazoles, with a hope that these new molecules would exhibit enhanced biological activity because of the presence of pharmacologically active heterocyclic and aromatic substituents. In our previous study, we have synthesized various heterocycles as antiinfective agents (Figure 1), where we determined that pyrrole and thiadiazole derivatives are good antitubercular and antimicrobial agents.[23–27] Keeping this in mind, we report here new prototype hybrid molecules (Figure 2) by combining pyrrole and thiadiazole

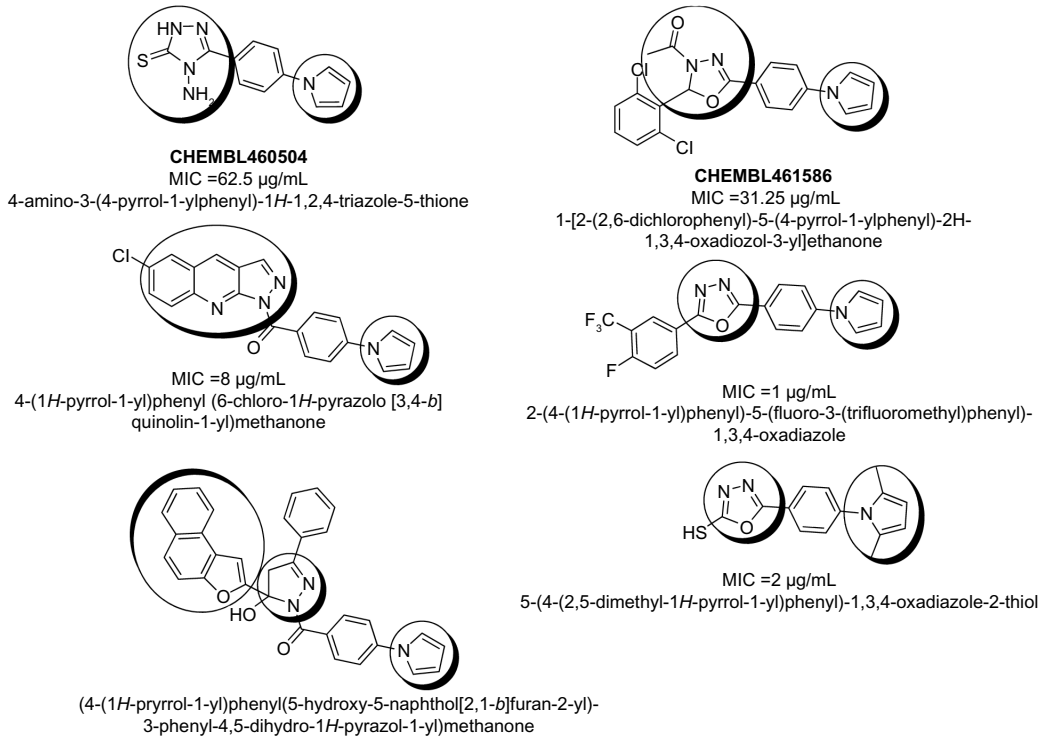

Figure 1 Reported molecules; pyrrole connected to heterocycles (oxadiazole, triazole, pyrazolo[3,4-*b*]quinolin-1-yl, naphtha[2,1-*b*]furan-2-yl) through phenyl bridge.
Abbreviations: CHEMBL, chemical database of bioactive molecules with drug-like properties; MIC, minimum inhibitory concentration.

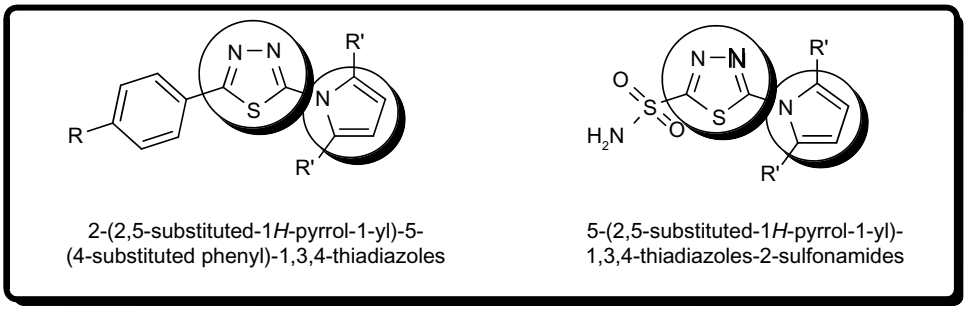

Figure 2 Designed molecules; pyrrole connected to thiadiazole directly.

moieties and investigating their in vitro antitubercular activity, as well as Surflex-Docking analyses. The present work, therefore reports on the structure and ligand-based drug design and discovery processes. The crystallographic 3D structural information of the biomolecular targets offers tremendous opportunities for establishing such novel drug design strategies to accelerate the drug discovery process. To accomplish this, docking simulation was performed to predict the binding orientation of small molecules to protein targets to predict their affinity and activity.[28]

Results and discussion

Synthesis and spectral studies

Compounds 4a–4i, 5a–5i, 8a, and 8b were synthesized as per Figures 3 and 4. In Figure 3, the 2-amino-5-(4-substituted phenyl)-1,3,4-thiadiazoles (3a–3i) were synthesized by condensation of aromatic acids (1a–i) with thiosemicarbazide (2) in the presence of a dehydration agent ($POCl_3$). The 2-amino-5-sulfonamido-1,3,4-thiadiazole (7) was obtained by the hydrolysis of acetazolamide (6) in concentrated HCl (Figure 4). The *Paal-Knorr* pyrrole synthesis involving

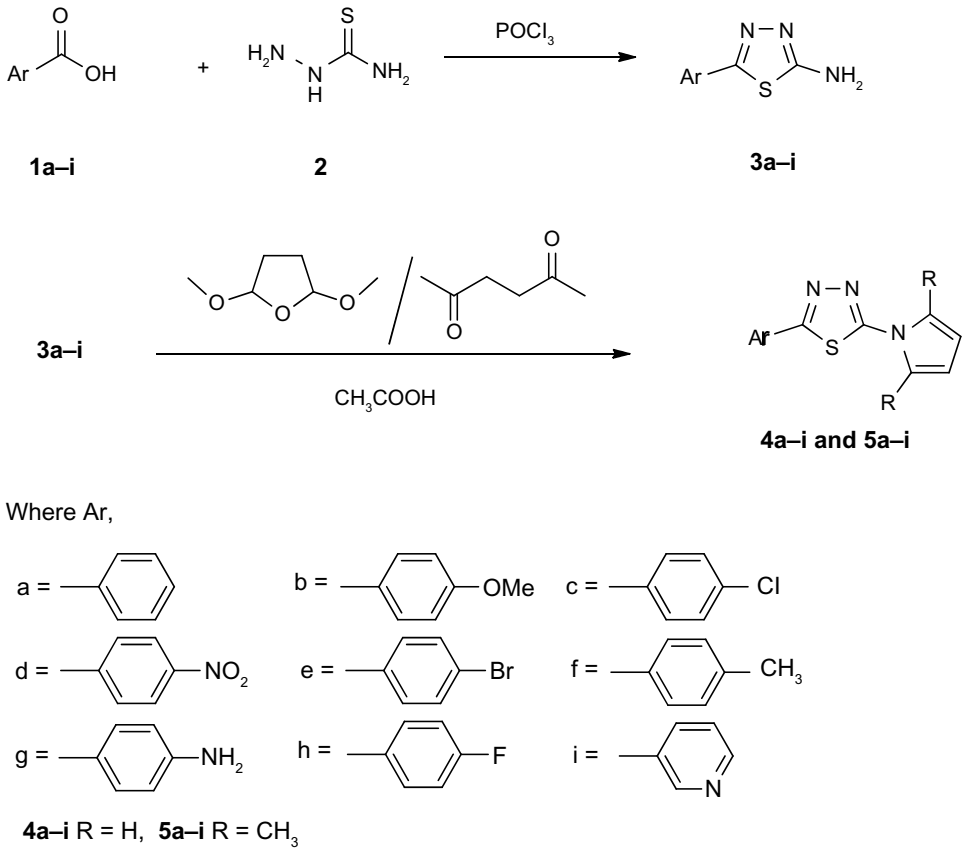

Figure 3 Synthetic route for 2-substituted pyrrole-1*H*-5-(4-substituted phenyl)-1,3,4-thiadiazoles.

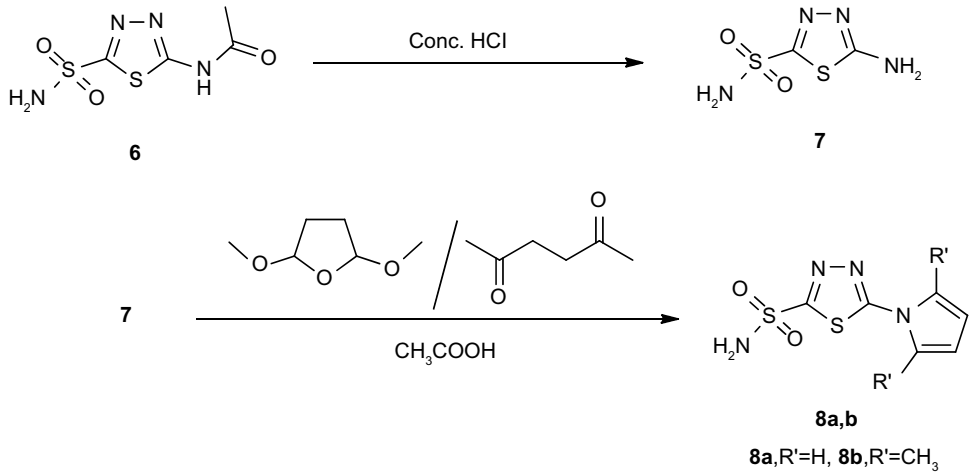

Figure 4 Synthetic route for 2-substituted pyrrole-1*H*-5-sulfonamido-1,3,4-thiadiazoles.
Abbreviation: Conc., concentration.

the reaction of 1,4-dicarbonyl (2,5-hexanedione) or 2,5-dimethoxy tetrahydrofuran with amines is among the most classical methods of heterocyclic pyrrole ring synthesis. Pyrrole (4a–4i, 8a) and 2,5-dimethyl pyrrole (5a–5i, 8b) rings have been constructed by using the free amino group at the second position of 1,3,4-thiadiazoles (3a–3i, 7) in the presence of dry glacial acetic acid.

Structures of the compounds were assigned by the spectral and analytical data; namely, Fourier transform infrared spectroscopy (FTIR), nuclear magnetic resonance (NMR), and mass spectroscopy, as reported in the experimental section. In the ^{1}H NMR spectrum of 4c, four protons of pyrrole moiety resonate as two doublet of doublets at δ 7.43 and δ 6.40, whereas four protons of phenyl moiety resonate as two doublets at δ 7.93 and δ 7.56. The mass spectrum of 4c showed the molecular ion peak at a mass-to-charge ratio (m/z) of 261.78 that confirmed its molecular weight.

The disappearance of the NH_2 stretching band in the FTIR spectrum of 5c confirmed the formation of dimethyl pyrrole. The ^{1}H NMR spectrum of 5c showed a singlet at δ 2.25 that was accounted for two methyl groups. The C_3 and C_4 protons of pyrrole ring appeared as a singlet at δ 5.94. The four protons of phenyl moiety resonate as two doublets at δ 8.02 and δ 7.60.

Electron impact mass spectra showed accurate molecular ion peaks at m/z 226.97, 257.49, 261.78 (263.78), 272.31 (273.31), 306.09 (308.09), 241.17, 242.28, 245.37, 228.11, 255.01, 285.11, 289.05 (291.05), 300.23 (301.23), 332.56 (334.56), 269.03, 270.17, 273.01, 256.13, 229.07, and 258.19 for compounds 4a–4i, 5a–5i, and 8a–8b, respectively.

Antitubercular activity

The results of antitubercular activities (expressed in minimum inhibitory concentration [MIC], which was converted to pMIC = –logMIC, calculated by Sybyl-X 2.0 software) of the compounds against selected *M. tuberculosis* $H_{37}Rv$ are illustrated in Table 1. The compounds (4a–4i, 5a–5i, and 8a–8b) showed the activities against mycobacteria, with the MIC values ranging from 12.5 to 100 μg/mL (pMIC 4.903–4.000). Compounds 4b, 5b, and 5d inhibited mycobacterial growth effectively compared with others in the series, showing MIC values of 12.5 μg/mL (pMIC 4.903), followed by compounds 4d, 4h, 4i, 5h, 5i, 8a, and 8b at 25 μg/mL (pMIC 4.602). The compounds with $-OCH_3$, $-NO_2$, -F, pyridine, and sulphonamide substituents have shown better antitubercular activities than others. In these compounds, all the functional groups are H-bond acceptors, which might be responsible for achieving a better inhibitory action on *M. tuberculosis*.

Protein quality and active site identification

Ramachandran plots, which give an indication of the quality of the model, as well as hydrophobicity plots (Figures 5 and 6A and B), were obtained at the end of the minimization. In Figure 5, red color violation 2 means PRO in the generously allowed region and non-GLY in the disallowed region, and a magenta color violation 1 means PRO in the allowed region and non-GLY in the generously allowed region, but a blue color violation 0 means PRO in the favored region, non-GLY in the favored or allowed region, and GLY in any region. Almost 98% of the residues were found in the most favored region, but 2% were found in the additional allowed regions; 0% were found in the disallowed regions. As shown

Table 1 Antimycobacterial activity (MIC values in µg/mL and pMIC values are –logMIC) for pyrrolyl thiadiazole derivatives (4a–4i, 5a–5i, and 8a–8b)

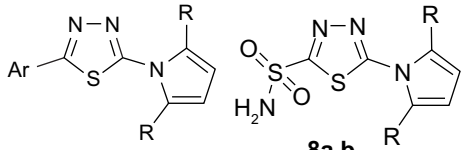

4a–i and 5a–i 8a,b

Compound	*Mycobacterium tuberculosis* $H_{37}Rv$ MIC (µg/mL)	pMIC* (–logMIC)
4a	100	4.000
4b	12.5	4.903
4c	100	4.000
4d	25	4.602
4e	100	4.000
4f	50	4.301
4g	50	4.301
4h	25	4.602
4i	25	4.602
5a	100	4.000
5b	12.5	4.903
5c	100	4.000
5d	12.5	4.903
5e	100	4.000
5f	50	4.301
5g	50	4.301
5h	25	4.602
5i	25	4.602
8a	25	4.602
8b	25	4.602
Isoniazid	0.25	6.6021

Note: *Values calculated by Sybyl-X 2.0 software.
Abbreviation: MIC, minimum inhibitory concentration.

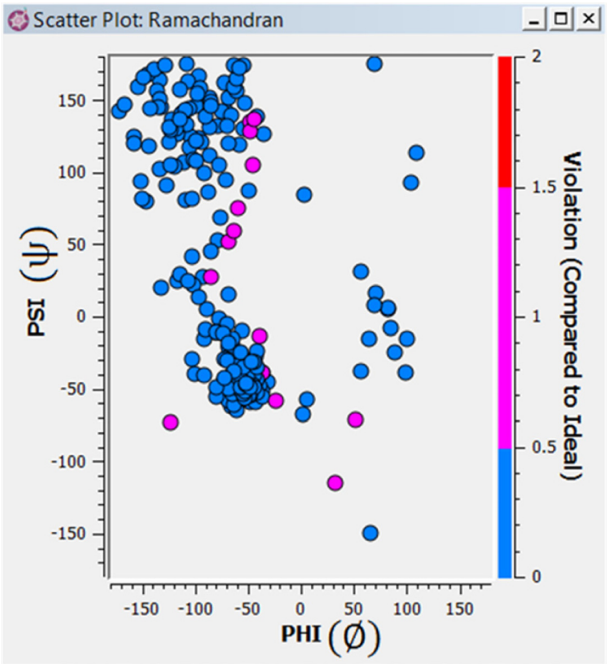

Figure 5 Ramachandran plot for analysis of residue shows the PHI (Φ) and PSI (ψ) torsion angles for all residues in structure; Φ values on X-axis and ψ values on Y-axis.
Notes: Red color indicates Proline (PRO) in generously allowed region and non-Glycine (GLY) in disallowed region; magenta color indicates PRO in allowed region and non-GLY in generously allowed region; blue color indicates PRO in favored region, non-GLY in favored or allowed region and GLY in any region.

in Figure 6A, analyzing the shape of the plot gives information about partial structure of the protein. For instance, if a stretch of about 20 amino acids shows positive for hydrophobicity, these amino acids may be part of alpha-helix spanning across a lipid bilayer, which is composed of hydrophobic fatty acids. On the converse, amino acids with high hydrophilicity indicate these residues are in contact with the solvent or water and are, therefore, likely to reside on the outer surface of the protein (scores are given in Table S1).

The active site at InhA was identified using SiteID or Protomol generation suite. The SiteID method generated many possible spheres of radius of water inside the protein molecules that were in search of the largest space or cluster available, which could be identified as an active site (Figure 7). A flood-fill algorithm, similar to the one implemented in CAVITY, was used[29] for each solvent molecule in the pocket, and all atoms in the protein lying within the specified distance (default =3 Å) were considered. This generated four sites: site 1, yellow, Gly96, Met103, Gly104, Pro156, Ala157, Tyr158, Met161, Met199, Ile202, Ile215, Leu218, and NAD500; site 2, green, Ile15, Ile16, NAD500, Leu38, Thr39, Gly40, Phe41, Ile47, Leu60, and Leu63; site 3, cyan, Phe149, Asp150, Met155, Ala190, Ala191, Trp222, and Asp261; and site 4, white, Ser19, His24, and Ala235. In the case of the Protomol method, Protomols can be produced by one of three routes: automatic: Surflex-Dock finds the largest cavity in the receptor protein; ligand-based: by a ligand in the same coordinate space as the receptor; residue-based: by specified residues in the receptor. Thus, a Protomol can be generated automatically or be defined on the basis of a cognate ligand or known active site. The sites generated were compared with the active site of the template and we found that site 1 (yellow region) is highly conserved. In this article, a Protomol generated by the ligand-based approach was identical to SiteID site 1. Hence, we used the ligand-based generated Protomol for further study (Figure 8A). However, Figure 8B gives a clear picture of the obtained active site.

Surflex-Dock was applied to studying the molecular docking, which uses an empirical scoring function and a patented search engine to dock the ligands into the protein's binding site.[30,31] In the docking procedure, ten binding poses per ligand were obtained, and the binding pose with the highest

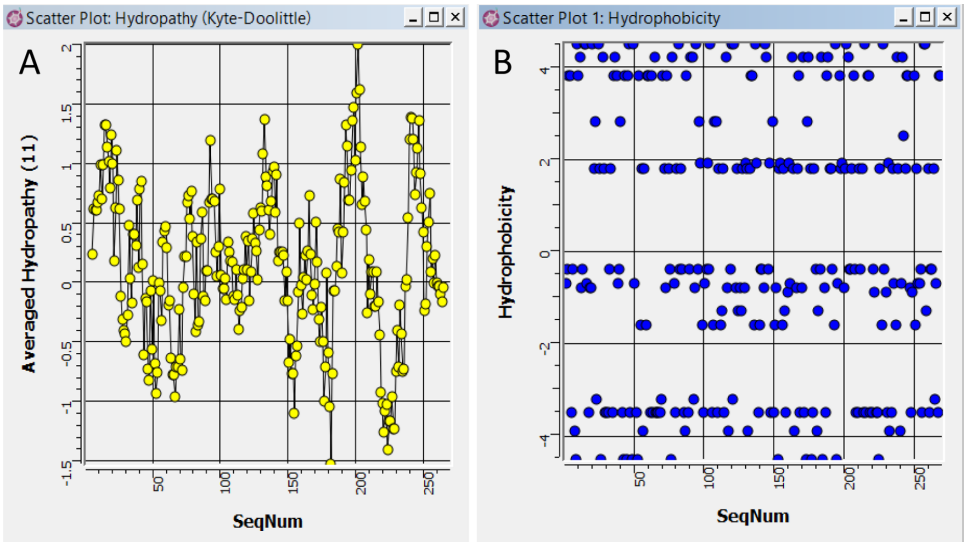

Figure 6 (**A**) Hydropathy index averaged over a moving window of eleven residues. (**B**) Hydrophobicity at each residue.

total score was considered for ligand–receptor interactions. Optimization of the results was carried out by allowing the protein movement. The strengths of the individual scoring functions were combined to produce a consensus that is more robust and accurate than any single function for evaluating the ligand–receptor interactions. Thus, CScore (consensus score) was used for ranking the affinity of ligands bound to the active site of a receptor. CScore integrates a number of popular scoring functions and provides several functions: D_Score, charge and van der Waals interactions between the protein and the ligand; PMF (potential of mean force) Score; G_Score, showing hydrogen bonding, complex (ligand–protein), and internal (ligand–ligand) energies; and Chem_Score, points for hydrogen bonding, lipophilic contact, and rotational entropy, along with an intercept term. CScore was automatically computed from the six scores (0, 1, 2, 3, 4, and 5); the best CScore is 5.

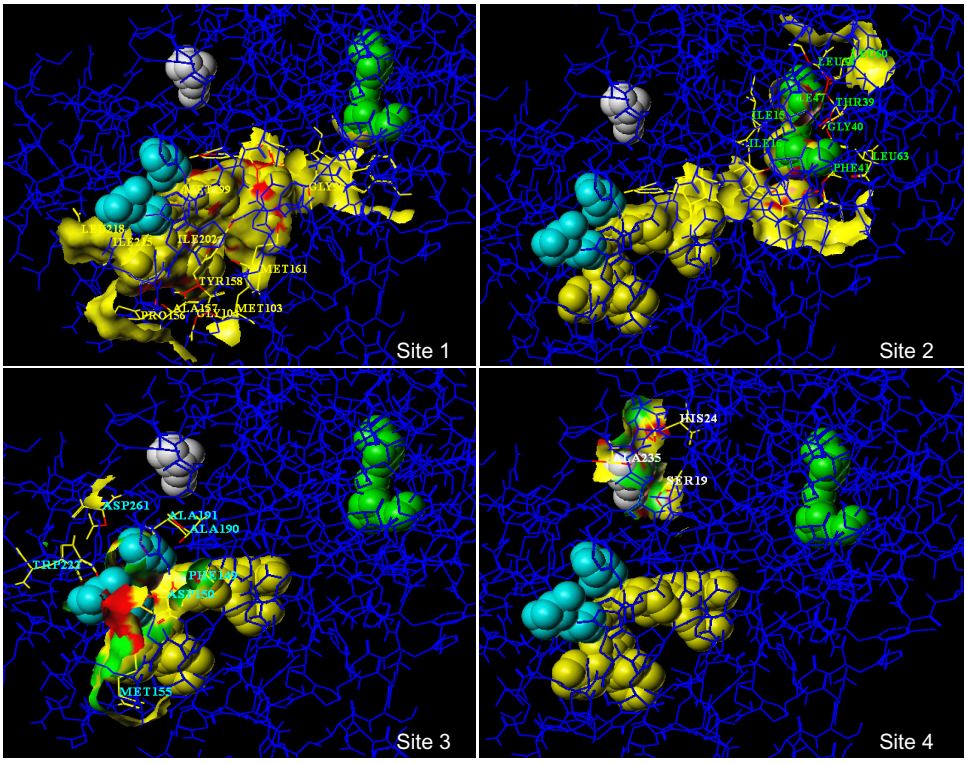

Figure 7 The possible binding-sites (spacefill models) of ENR enzyme from *Mycobacterium tuberculosis*; site 1, yellow; site 2, green; site 3, cyan; site 4, white.

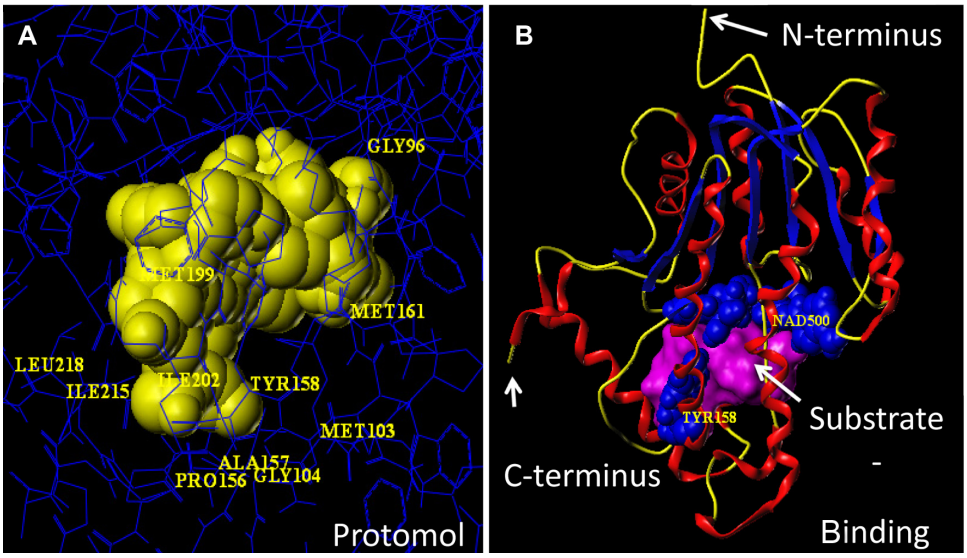

Figure 8 (**A**) Protomol generated (yellow-colored spacefill model) at ENR enzyme, using a ligand-based approach and (**B**) active site at ENR enzyme (Tyr158 and NAD^+ spacefill models in blue; magenta, Connolly surface; ribbon colored by secondary structure).

Structures with scores of 3 or 4 merit further consideration. Structures with a CScore of 0 are consistently considered bad by all scoring functions and should be dropped. Additional scores were observed as we allowed the protein movement.

Surflex-Docking

Docking simulation plays a key role in structural molecular biology and computer-assisted drug designing. Binding models for receptors and ligands via the lowest energy pathway may be best represented by docking simulations. One of the most effective docking techniques is Surflex-Dock. The literature review showed that Surflex-Dock has several advantages in drug design studies.

In our previous communication, protein flexibility was not considered,[17] and hence, in the present study, we have investigated the effect of protein flexibility on the docking process. To accomplish this process, the protein movement was allowed, which means whether to allow flexibility of protein atoms whose van der Waals surface distances from ligand atoms are less than 4 Å and to adapt the active site conformation to the docked ligand. Only hydrogens were allowed in protein flexibility to optimize hydroxyls and thiols,

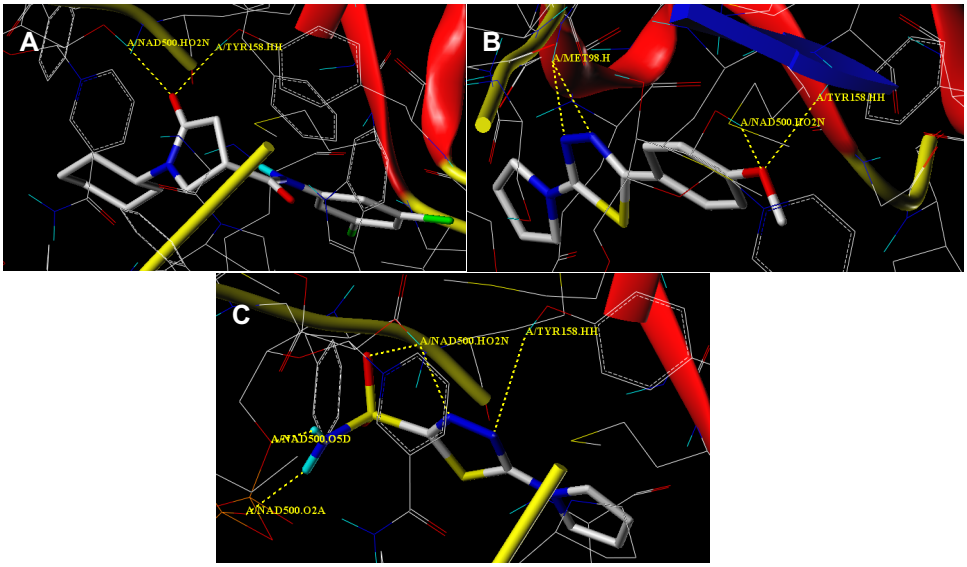

Figure 9 Docking conformation (capped sticks model in atom type color) of 641 (**A**), compounds 4b (**B**), and 8a (**C**) at the active site (yellow dotted lines indicate H-bond); flexible docking.

as well as all protons in the protein pocket. The binding models of 641, 4b, and 8a are depicted in Figure 9A–C. Model 641 showed two H-bonding interactions; the oxygen of the carbonyl group on pyrrolidine makes H-bonds with that of the OH group of the active site of Tyr158 (2.12 Å) and NAD^+ ribose (1.95 Å). Compound 4b makes four hydrogen bonds: the oxygen atom of the methoxy group makes two H-bonds with Tyr158 (2.23 Å) and NAD^+ ribose (1.82 Å), and that of nitrogens at the third and fourth positions of the oxadiazole ring makes two H-bonds with Met98 (1.97 and 2.29 Å). In the case of compound 8a, it makes five H-bonds; that is, at the third position nitrogen (Tyr158, 2.88 Å) and the fourth position nitrogen (NAD^+ ribose, 2.21 Å) of the oxadiazole ring, compound 8a makes two H-bonds. Free NH_2 of sulphonamide group makes two H-bonds with NAD^+ ribose (2.04 and 1.91 Å), and one more H-bond was observed between NAD^+ ribose and the oxygen of SO_2 with a distance of 2.42 Å. However, in the case of nonprotein flexibility (compounds 641, 4b, and 8a), the H-bonding interactions at the active site with their respective distances are given in Table 2. The binding models of 641, 4b, and 8a by nonprotein flexibility docking are depicted in Figures 10–12.

Furthermore, interactions were also stabilized by the hydrophobic residues of the inner cavity, such as in Ile16, Ile21, Phe97, Met98, Pro99, Met103, Pro156, Ala157, Typ160, Met161, Pro193, and Ile194 and hydrophilic residues such as Gly14, Ser19, Ser20, Ser94, Gly96, Gln100, Gly102, Gly104, Gly119, Asp148, Asp150, Tyr158, Asn159, Thr162, Gly192, and Thr196. These amino acid residues were involved in the active cavity (shown in Figure 13A and B). Pmove score, the average movement of the protein atoms in the pocket for this pose, was observed in the range of 0.08–0.12, but not much change was observed when it was aligned with both the models. The docking scores, namely, C-score, Crash, Polar, D_Score, PMF_Score, G_Score, and Chem_Score, from Surflex-Dock are given in Tables 3 and 4. None of the molecules were observed with better scores than the re-docked 641 ligand, but they are making key interactions at the active site or substrate binding site. Comparing the predicted (CScore) and experimental (pMIC) results, it can be said that compounds with pMIC values of 4.903 and 4.602 showed the highest CScores (6.36–5.45) compared with other molecules in the series.

Experimental

All chemicals used were purchased either from Sigma-Aldrich, Fine-Chem Limited, or Spectrochem Pvt Ltd. Solvents were of reagent grade, and whenever necessary, they were purified and dried using the standard methods.

Table 2 Key H-bonding interactions observed by simple and flexible docking processes with distance in Å.

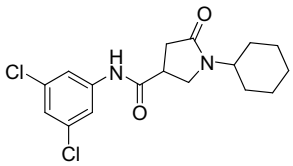

1-Cyclohexyl-*N*-(3,5-dichlorophenyl)-5-oxopyrrolidine-3-carboxamide (pyrrolidine carboxamide or 641)

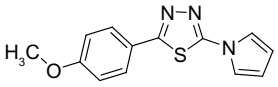

4b

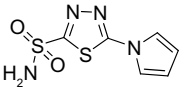

8a

Compound	Protein Flexibility	Å	Simple (Base)	Å
641	Pyrrolidine C=O–NAD^+	1.95	Pyrrolidine C=O–NAD^+	1.91
	Pyrrolidine C=O–Tyr158	2.12	Pyrrolidine C=O–Tyr158	2.07
4b	CH_3O–Tyr158	2.23	CH_3O–Met98	2.04
	CH_3O–NAD^+	1.82	Oxadiazole 3rd N–Tyr158	2.25
	Oxadiazole 3rd N–Met98	1.97	Oxadiazole 3rd N–NAD^+	2.15
	Oxadiazole 4th N–Met98	2.29	Oxadiazole 4th N–Tyr158	2.74
			Oxadiazole 4th N–NAD^+	2.44
8a	Oxadiazole 3rd N–Tyr158	2.88	HNH–NAD^+	2.53
	Oxadiazole 4th N–NAD^+	2.21	OSO–Tyr158	2.09
	HNH–NAD^+	2.04	OSO–NAD^+	2.22
	HNH–NAD^+	1.91		
	OSO–NAD^+	2.42		

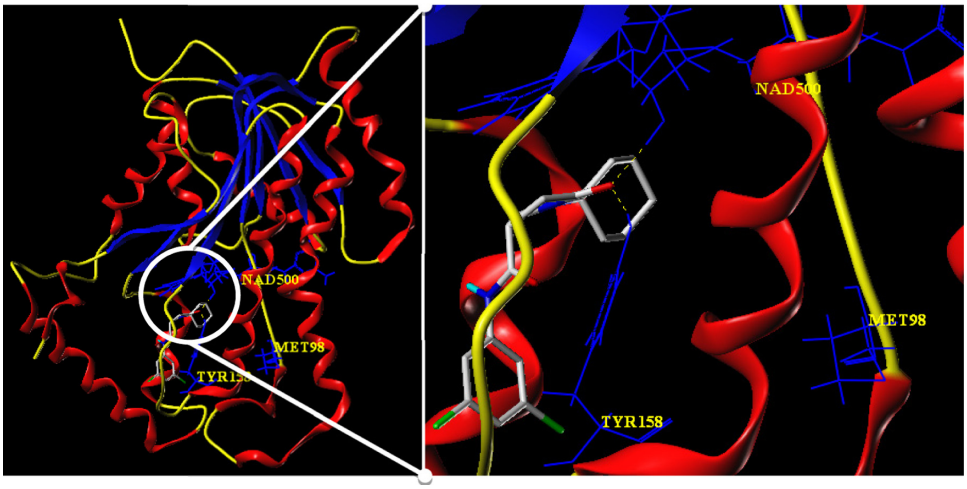

Figure 10 Docking conformation of 641 (capped sticks model in atom type color) at the active site (yellow dotted lines indicate H-bond).

The melting points of the compounds were determined using the Shital Scientific Industries melting point apparatus and are uncorrected. FTIR spectra were recorded on a Bruker spectrophotometer, using KBr pellets. The ^{1}H and ^{13}C NMR spectra were recorded on a Bruker AVANCE II 400 MHz instrument, using dimethyl sulfoxide (DMSO)-d_6 solvent and TMS as the internal standard. Chemical shifts are expressed in δ values (ppm).

Mass spectra (MS) were taken in JEOL GCMATE II GC-Mass and Waters Micromass Q-Tof Micro liquid chromatography-mass spectrometers. The compounds showed spectral data consistent with their proposed. Analytical thin-layer chromatography (TLC) was performed on precoated TLC sheets of silica gel 60 F_{254} (Merck, Darmstadt, Germany), visualized by long- and short-wavelength ultraviolet lamps. Chromatographic purifications were performed on Merck aluminum oxide (70–230 mesh) and Merck silica gel (70–230 mesh).

General procedure for the preparation of 2-amino-5-(4-substituted phenyl)-1,3,4-thiadiazoles (3a–3i)

A mixture of appropriate aromatic acid (50 mmol), *N*-aminothiourea (50 mmol), and $POCl_3$ (13 mL) was heated at 75°C for 30 minutes and cooled, to which 10 mL of water was added, and the mixture was refluxed for 4 hours. The pH was then adjusted to 8.0 by adding 50% sodium hydroxide solution. The separated solid was filtered and recrystallized from ethanol to give the desired compounds.[32]

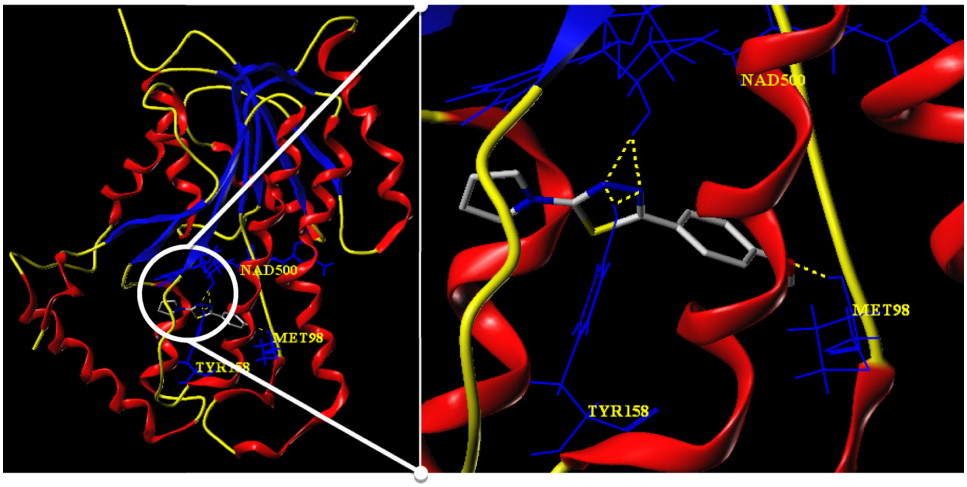

Figure 11 Docking conformation of compound 4b (capped sticks model in atom type color) at the active site (yellow dotted lines indicate H-bond).

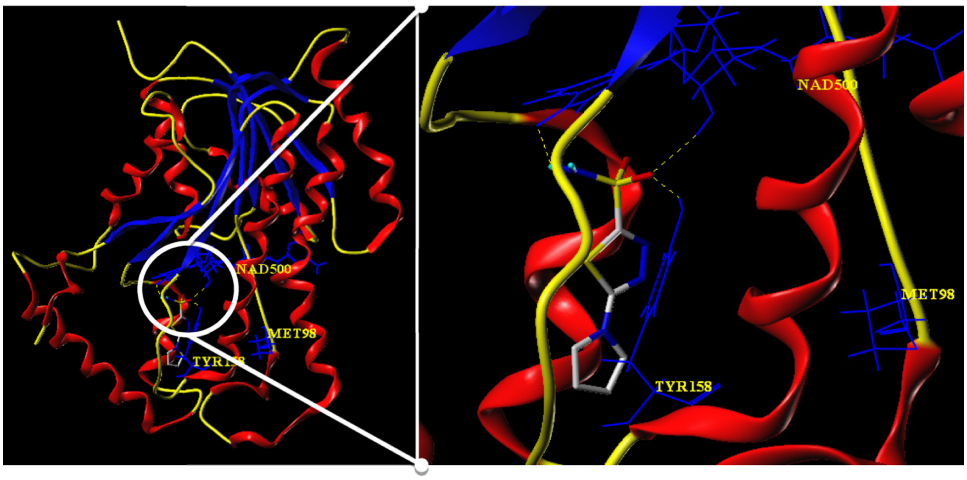

Figure 12 Docking conformation of compound 8a (capped sticks model in atom type color) at the active site (yellow dotted lines indicate H-bond).

General procedure for the preparation of 5-(4-substituted phenyl)-2-(1*H*-pyrrol-1-yl) 1-1,3,4-thiadiazoles (4a–4i)

To a solution of 2-amino-5-(4-substituted phenyl)-1,3,4-thiadiazoles (10 mmol) in 20 mL glacial acetic acid, 2,5-dimethoxytetrahydrofuran (15 mmol) was added slowly at room temperature and refluxed for 1 hour (monitored by TLC). The reaction mixture was poured into ice-cold water and basified with sodium bicarbonate solution. The separated solid was collected, washed with water, and dried. All the compounds were recrystallized, using ethanol as the solvent.

4-Phenyl-5-(1*H*-pyrrol-1-yl)-1,3,4-thiadiazole (4a)

Yield, 78%: mp 136°C–138°C; FTIR (KBr): 2,923 and 2,848 (Ar-H), 1,509 (C=N) cm^{-1}; ^1H NMR (400 MHz, deuterated chloroform [$CDCl_3$]) δ ppm: 6.44 (s, 2H, pyrrole-C_3, and C_4-H), 7.55 (dd, 2H, pyrrole-C_2 and C_5-H), 7.57–7.59 (m, 3H, ph-C_3, C_4, C_5-H), 7.95 (d, 2H, ph-C_2, and C_6-H); ^{13}C NMR (400 MHz, $CDCl_3$) δ ppm: 113.54 (pyrrole-C_3 and C_4), 121.66 (pyrrole-C_2 and C_5), 127.68 (ph-C_2 and C_6), 129.82 (ph-C_4), 129.99 (ph-C_3 and C_5), 131.85 (ph-C_1), 162.22 (thiadiazole-C_2), 164.24 (thiadiazole-C_5); MS (EI): m/z = found 226.97 [M^+]; calcd. 227.05. Anal. $C_{12}H_9N_3S$.

2-(4-Methoxyphenyl)-5-(1*H*-pyrrol-1-yl)-1,3,4-thiadiazole (4b)

Yield, 71%: mp 140°C–142°C; FTIR (KBr): 2,926 and 2,836 (Ar-H), 1,605 (C=N) cm^{-1}; ^1H NMR (500 MHz, $CDCl_3$) δ ppm: 3.87 (s, 3H, OCH_3), 6.39 (dd, 2H, pyrrole-C_3, and C_4-H), 7.05 (dd, 2H, ph-C_3, and C_5-H), 7.39 (dd, 2H, pyrrole-C_2, and C_5-H), 7.86 (dd, 2H, ph-C_2, and C_6-H); ^{13}C NMR (300 MHz, DMSO) δ ppm: 55.27 (OCH_3), 112.65 (pyrrole-C_3 and C_4), 114.56 (ph-C_3 and C_5), 120.72 (pyrrole-C_2 and C_5), 121.83 (ph-C_1), 128.65 (ph-C_2 and C_6), 160.75 (ph-C_4), 161.52 (thiadiazole-C_2), 163.32 (thiadiazole-C_5); MS (EI): m/z = found 257.49 [M^+]; calcd. 257.31. Anal. $C_{13}H_{11}N_3OS$.

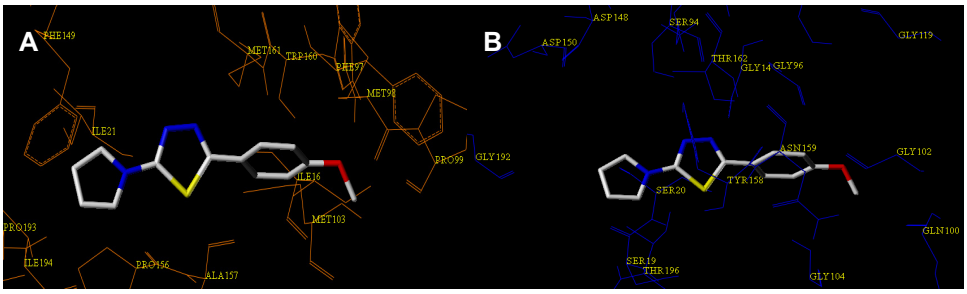

Figure 13 Hydrophobic (brown) (**A**) and hydrophilic (blue) (**B**) amino acids surrounded to compound 4b (capped sticks model in atom type color).

Table 3 Surflex-Dock scores of pyrrolyl thiadiazole derivatives

Compound	CScore	Crash	Polar	Strain	Total	Ligmin	Full	Complex	Cscale	Pmove
641	9.38	–2.013	2.084	0.562	8.819	50.758	39.556	463.670	132.919	0.1004
4b	6.36	–0.393	2.552	1.105	4.717	48.173	42.111	457.829	128.903	0.1138
8a	6.31	–0.532	2.928	0.201	5.628	62.202	54.658	473.731	76.408	0.1230
5d	5.85	–0.492	1.439	0.985	4.607	56.286	50.581	471.206	124.398	0.1089
8b	5.82	–1.890	0.900	2.319	3.997	70.449	65.082	486.675	93.730	0.0825
5i	5.82	–0.940	1.175	3.629	1.821	50.409	48.879	472.224	112.434	0.0946
5b	5.59	–0.581	1.837	0.914	4.438	56.254	50.297	465.651	169.768	0.1158
4d	5.45	–1.039	2.863	0.894	3.650	48.203	43.276	461.266	102.927	0.0989
5f	5.35	–1.012	0.0002	6.269	–0.952	53.402	56.588	486.345	110.978	0.1031
5h	5.35	–1.615	1.911	3.021	2.237	51.148	49.186	474.273	112.233	0.1100
4i	5.31	–0.697	1.977	1.046	4.018	42.317	37.691	459.429	91.126	0.1221
4f	5.25	–0.693	0.000	0.892	3.952	45.323	41.371	466.987	90.803	0.1032
4h	5.09	–1.136	2.025	1.544	3.221	43.069	39.179	462.690	92.538	0.1171
5c	5.06	–1.133	0.325	0.189	4.643	51.107	44.841	467.786	106.628	0.1082
4a	4.84	–0.771	1.999	1.924	3.429	42.925	38.731	461.707	93.086	0.1129
5g	4.83	–1.013	1.166	2.067	4.297	51.661	46.173	469.797	108.415	0.1023
4g	4.76	–0.454	1.203	2.440	3.418	43.582	40.183	465.136	87.213	0.1121
5a	4.58	–1.254	0.000	2.975	2.120	51.004	48.346	470.792	108.915	0.1102
4e	4.54	–0.735	0.000	0.056	4.524	42.528	36.420	458.667	86.869	0.0965
5e	4.33	–1.404	0.000	0.343	3.987	50.607	45.235	467.265	112.289	0.0872
4c	3.65	–0.434	0.007	0.573	3.0811	43.028	39.913	459.516	99.895	0.1008

Notes: CScore, consensus score, integrates a number of popular scoring functions for ranking the affinity of ligands bound to the active site of a receptor and reports the output of total score; Crash, the degree of inappropriate penetration by the ligand into the protein and of interpenetration (self-clash) between ligand atoms that are separated by rotatable bonds (crash scores close to 0 are favorable, negative numbers indicate penetration); Polar, contribution of the polar interactions to the total score; Pose, indication of which pose in the initial run has the best score after optimization with protein flexibility; Strain, nominal ligand strain relative to the nearby local minimum in units of pKd; Total, ligand's score corrected for strain energy; Ligmin, energy of the nearby ligand minimum (kcal/mol); Full, absolute energy of the optimized ligand, including protein interaction (kcal/mol); Complex, absolute energy of the complex including ligand, protein pocket, and intermolecular interactions (kcal/mol); Cscale, scaled complex score that normalizes the protein score components so that ligand poses that contact different numbers of protein atoms are more directly comparable; Pmove, average movement of the protein atoms in the pocket for this pose.

2-(4-Chlorophenyl)-5-(1*H*-pyrrol-1-yl)-1,3,4-thiadiazole (4c)

Yield, 89%: mp 160°C–162°C; FTIR (KBr): 2,918 and 2,848 (Ar-H), 1,584 (C=N) cm^{-1}; ^1H NMR (400 MHz, $CDCl_3$) δ ppm: 6.40 (dd, 2H, pyrrole-C_3, and C_4-H), 7.43 (dd, 2H, pyrrole-C_2, C_5-H), 7.56 (dd, 2H, ph-C_3, C_5-H), 7.93 (dd, 2H, ph-C_2, C_6-H); ^{13}C NMR (400 MHz, $CDCl_3$) δ ppm: 113.62 (pyrrole-C_3 and C_4), 121.69 (pyrrole-C_2 and C_5), 128.68 (ph-C_2 and C_6), 129.36 (ph-C_3 and C_5), 130.05 (ph-C_1), 136.42 (ph-C_4), 162.50 (thiadiazole-C_2), 163.05 (thiadiazole-C_5); MS (electrospray ionisation [EI]): m/z = found 261.78 [M^+], 263.78 [M^+ +2]; calcd. 261.73. Anal. $C_{12}H_8ClN_3S$.

2-(4-Nitrophenyl)-5-(1*H*-pyrrol-1-yl)-1,3,4-thiadiazole (4d)

Yield, 63%: mp 216°C–219°C; FTIR (KBr): 2,916, 2,848 (Ar-H), 1,600 (C=N), 1,503, 1,339 (NO_2) cm^{-1}; ^1H NMR (400 MHz, $CDCl_3$) δ ppm: 6.44 (dd, 2H, pyrrole-C_3, and C_4-H), 7.54 (dd, 2H, pyrrole C_2, and C_5-H), 8.23 (dd, 2H, ph-C_2, and C_6-H), 8.41 (dd, 2H, ph-C_3, and C_5-H); ^{13}C NMR (400 MHz, $CDCl_3$) δ ppm: 113.27 (pyrrole-C_3 and C_4), 121.12 (pyrrole-C_2 and C_5), 124.48 (ph-C_3 and C_5), 128.28 (ph-C_2 and C_6), 134.99 (ph-C_1), 148.58 (ph-C_4), 161.39 (thiadiazole-C_2), 162.89 (thiadiazole-C_5); MS (EI): m/z = found 272.31 [M^+], 273.31 [M^++1]; calcd. 272.28. Anal. $C_{12}H_8N_4O_2S$.

2-(4-Bromophenyl)-5-(1*H*-pyrrol-1-yl)-1,3,4-thiadiazole (4e)

Yield, 58%: mp 162°C–165°C; FTIR (KBr): 2,919 and 2,847 (Ar-H), 1,581 (C=N), 598 (C-Br) cm^{-1}; ^1H NMR (400 MHz, $CDCl_3$) δ ppm: 6.42 (dd, 2H, pyrrole-C_3, and C_4-H), 7.49 (dd, 2H, pyrrole C_2, and C_5-H), 7.75 (dd, 2H, ph-C_2, and C_6-H), 7.88 (dd, 2H, ph-C_3, and C_5-H); ^{13}C NMR (400 MHz, $CDCl_3$) δ ppm: 114.12 (pyrrole-C_3 and C_4), 122.02 (pyrrole-C_2 and C_5), 125.61 (ph-C_3 and C_5), 129.15 (ph-C_2 and C_6), 141.11 (ph-C_1), 150.02 (ph-C_4), 162.77 (thiadiazole-C_2), 164.03 (thiadiazole-C_5); MS (EI): m/z = found 306.09 [M^+], 308.09 [M^+ +2]; calcd. 306.18. Anal. $C_{12}H_8BrN_3S$.

Table 4 Different energy scores for pyrrolyl thiadiazole derivatives from the Surflex-Docking

Compound	D_Score	PMF_Score	G_Score	Chem_Score
641	−165.064	−47.432	−307.404	−40.847
4b	−94.264	−23.652	−160.044	−30.804
8a	−82.683	−19.103	−144.253	−21.664
5d	−110.202	−41.217	−205.635	−33.361
8b	−111.536	−29.986	−223.381	−24.604
5i	−107.782	−37.474	−190.661	−28.107
5b	−87.341	−5.795	−159.397	−23.627
4d	−106.140	−35.445	−190.190	−30.956
5f	−112.667	−49.694	−201.966	−31.949
5h	−113.189	−37.517	−200.604	−30.856
4i	−98.115	−62.598	−174.071	−30.076
4f	−107.354	−48.404	−206.646	−28.704
4h	−102.147	−56.944	−171.950	−31.937
5c	−118.211	−37.568	−232.891	−34.055
4a	−102.014	−55.794	−182.947	−32.481
5g	−114.026	−46.381	−224.167	−34.071
4g	−104.048	−60.144	−201.189	−30.929
5a	−112.160	−40.039	−226.546	−32.848
4e	−111.801	−42.087	−212.967	−31.842
5e	−110.293	−33.448	−205.215	−30.056
4c	−97.889	−31.368	−177.013	−28.136

Notes: D_Score, charge and van der Waals interactions between the protein and the ligand; PMF_Score, indicating the Helmholtz free energies of interactions for protein–ligand atom pairs; PMF, potential of mean force; G_Score, showing hydrogen bonding, complex (ligand–protein), and internal (ligand–ligand) energies; Chem_Score, points for hydrogen bonding, lipophilic contact, and rotational entropy, along with an intercept term.

2-(4-Methylphenyl)-5-(1*H*-pyrrol-1-yl)-1,3,4-thiadiazole (4f)

Yield, 83%: mp174°C–176°C; FTIR (KBr): 2,917, 2,863 (Ar-H), 1,593 (C=N) cm^{-1}; ^1H NMR (400 MHz, $CDCl_3$) δ ppm: 2.41 (s, 3H, CH_3), 6.39 (s, 2H, pyrrole-C_3, and C_4-H), 7.34 (d, 2H, $J = 4.90$ ph-C_2 and C_6-H), 7.43 (s, 2H, $J = 4.92$ pyrrole C_2 and C_5-H), 7.81 (d, 2H, ph-C_3, and C_5-H); ^{13}C NMR (400 MHz, $CDCl_3$) δ ppm: 27.33 (CH_3), 112.36 (pyrrole-C_3 and C_4), 120.93 (pyrrole-C_2 and C_5), 126.03 (ph-C_3 and C_5), 128.23 (ph-C_2 and C_6), 143.12 (ph-C_1), 148.56 (ph-C_4), 161.87 (thiadiazole-C_2), 163.35 (thiadiazole-C_5); MS (EI): m/z = found 241.17 [M^+]; calcd. 241.07. Anal. $C_{13}H_{11}N_3S$.

2-(4-Aminophenyl)-2-(1*H*-pyrrol-1-yl)-1,3,4-thiadiazole (4g)

Yield, 20%: mp 180°C–182°C; FTIR (KBr): 3,381 (NH_2), 2,923, 2,853 (Ar-H), 1,603 (C=N) cm^{-1}; ^{1}HNMR (400 MHz, $CDCl_3$) δ ppm: 6.33 (dd, 2H, pyrrole-C_3, and C_4-H), 6.42 (s, 2H, NH_2), 7.35 (dd, 2H, pyrrole C_2, and C_5-H), 7.44–7.7.77 (m, 4H, ph-C_2, C_3, C_5, and C_6-H); ^{13}C NMR (400 MHz, $CDCl_3$) δ ppm: 114.13 (pyrrole-C_3 and C_4), 123.00 (pyrrole-C_2 and C_5), 126.05 (ph-C_3 and C_5), 128.66 (ph-C_2 and C_6), 140.59 (ph-C_1), 149.55 (ph-C_4), 162.25 (thiadiazole-C_2), 164.12 (thiadiazole-C_5); MS (EI): m/z = found 242.28 [M^+]; calcd. 242.30. Anal. $C_{12}H_{10}N_4S$.

2-(4-Fluorophenyl)-5-(1*H*-pyrrol-1-yl)-1,3,4-thiadiazole (4h)

Yield, 62%: mp 149°C–151°C; FTIR (KBr): 2,918 and 2,848 (Ar-H), 1,594 (C=N) cm^{-1}; ^1H NMR (400 MHz, $CDCl_3$) δ ppm: 6.40 (dd, 2H, pyrrole-C_3, and C_4-H), 7.33 (dd, 2H, pyrrole-C_2, and C_5-H), 7.44 (dd, 2H, ph-C_3, and C_5-H), 7.98 (dd, 2H, ph-C_2, and C_6-H); ^{13}C NMR (400 MHz, $CDCl_3$) δ ppm: 112.79 (pyrrole-C_3 and C_4), 116.13 (ph-C_3 and C_5), 120.69 (pyrrole-C_2 and C_5), 129.24 (ph-C_2 and C_6), 129.33 (ph-C_1), 161.50 (thiadiazole-C_2), 162.26 (ph-C_4), 164.92 (thiadiazole-C_5); MS (EI): m/z = found 245.37[M^+]; calcd. 245.28. Anal. $C_{12}H_8FN_3S$.

2-(Pyridin-3-yl)-5-(1*H*-pyrrol-1-yl)-1,3,4-thiadiazole (4i)

Yield, 61%: mp 136°C–138°C; FTIR (KBr): 2,988 and 2,923 (Ar-H), 1,597 (C=N) cm^{-1}; ^1H NMR (400 MHz, $CDCl_3$) δ ppm: 6.42 (dd, 2H, pyrrole-C_3, and C_4-H), 7.35 (dd, 2H, pyrrole-C_2, and C_5-H), 7.56–9.01 (m, 4H, pyridine-C_2, C_4-H, C_5-H, and C_6-H); ^{13}C NMR (400 MHz, $CDCl_3$) δ ppm: 109.05 (pyrrole-C_3 and C_4), 124.26 (pyridine-C_5), 130.02 (pyrrole-C_2 and C_5), 133.54 (pyridine-C_3), 134.06 (pyridine-C_4), 148.23 (pyridine-C_6), 149.08 (pyridine-C_2), 163.39 (thiadiazole-C_2), 174.57 (thiadiazole-C_5); MS (EI): m/z = found 228.11 [M^+]; calcd. 228.05. Anal. $C_{11}H_8N_4S$.

General procedure for the preparation of 5-(4-substituted phenyl)-2-(2,5-dimethyl-1*H*-pyrrol-1-yl)-1,3,4-thiadiazoles (5a–5i)

To a solution of 2-amino-4-(4-substituted phenyl) thiadiazoles (10 mmol) in 20 mL glacial acetic acid, acetonyl acetone (15 mmol) was added slowly at room temperature and refluxed for 1 hour (monitored by TLC). This mixture was poured into ice-cold water and basified with sodium bicarbonate solution. The separated solid was collected, washed with water, dried, and recrystallized, using n-hexane as the solvent.

2-(2,5-Dimethyl-1*H*-pyrrol-1-yl)-5-phenyl-1,3,4-thiadiazole (5a)

Yield, 58%: mp 234°C–238°C; FTIR (KBr): 2,951 and 2,853 (Ar-H), 1,624 (C=N) cm^{-1}; 1H NMR (400 MHz, $CDCl_3$) δ ppm: 2.28 (s, 6H, $2CH_3$), 5.94 (s, 2H, pyrrole-C_3 and C_4-H),

7.37–7.44 (m, 3H, ph-C_3, C_4 and C_5-H), 7.74–7.77 (m, 2H, ph-C_2 and C_6-H); ^{13}C NMR (400 MHz, $CDCl_3$) δ ppm: 13.01 (2 CH_3), 111.24 (pyrrole-C_3 and C_4), 128.21 (pyrrole-C_2 and C_5), 129.57 (ph-C_2 and C_6), 132.08 (ph-C_3 and C_5), 132.90 (ph-C_1), 135.29 (ph-C_4), 162.06 (thiadiazole-C_2), 164.03 (thiadiazole-C_5); MS (EI): m/z = found 255.01 [M^+]; calcd. 255.08. Anal. $C_{14}H_{13}N_3S$.

2-(4-Methoxyphenyl)-5-(2,5-dimethyl-1*H*-pyrrol-1-yl)-1,3,4-thiadiazole (5b)

Yield, 38%: mp 110°C–112°C; FTIR (KBr): 2,922 and 2,845 (Ar-H), 1,606 (C=N) cm^{-1}; ^{1}H NMR (400 MHz, $CDCl_3$) δ ppm: 2.24 (s, 6H, 2CH_3), 3.88 (s, 3H, OCH_3), 5.92 (s, 2H, pyrrole-C_3 and C_4-H), 7.10 (dd, 2H, ph-C_3 and C_5-H), 7.94 (dd, 2H, ph-C_2 and C_6-H); ^{13}C NMR (400 MHz, $CDCl_3$) δ ppm: 12.90 (2CH_3), 55.26 (OCH_3), 108.60 (pyrrole-C_3 and C_4), 114.54 (ph-C_3 and C_5), 121.93 (pyrrole-C_2 and C5), 129.28 (ph-C_2 and C_6), 128.92 (ph-C_1), 158.52 (ph-C_4), 161.79 (thiadiazole-C_2), 168.17 (thiadiazole-C_5); MS (EI): m/z = found 285.11 [M^+]; calcd. 285.09. Anal. $C_{15}H_{15}N_3OS$.

2-(4-Chlorophenyl)-5-(2,5-dimethyl-1*H*-pyrrol-1-yl)-1,3,4-thiadiazole (5c)

Yield, 42%: mp 128°C–130°C; FTIR (KBr): 2,917 and 2,852 (Ar-H), 1,590 (C=N) cm^{-1}; ^{1}H NMR (400 MHz, $CDCl_3$) δ ppm: 2.25 (s, 6H, 2CH_3), 5.94 (s, 2H, pyrrole-C_3 and C_4-H), 7.60 (dd, 2H, ph-C_3 and C_5-H), 8.02 (dd, 2H, ph-C_2 and C_6-H); ^{13}C NMR (400 MHz, $CDCl_3$) δ ppm: 13.00 (2CH_3), 108.90 (pyrrole-C_3 and C_4), 128.16 (pyrrole-C_2 and C_5), 128.85 (ph-C_2 and C_6), 129.34 (ph-C_3 and C_5), 129.38 (ph-C_1), 136.50 (ph-C_4), 159.67 (thiadiazole-C_2), 166.99 (thiadiazole-C_5); MS (EI): m/z = found 289.05 [M^+], 291.05 [M^+ +2]; calcd. 289.04. Anal. $C_{14}H_{12}ClN_3S$.

2-(4-Nitrophenyl)-5-(2,5-dimethyl-1*H*-pyrrol-1-yl)-1,3,4-thiadiazole (5d)

Yield, 43%: mp 150°C–152°C; FTIR (KBr): 2,921 and 2,854 (Ar-H), 1,596 (C=N), 1,497, 1,331 (NO_2) cm^{-1}; ^{1}H NMR (500 MHz, $CDCl_3$) δ ppm: 2.30 (s, 6H, 2CH_3), 5.96 (s, 2H, pyrrole-C_3 and C_4-H), 8.28 (d, 2H, J = 8.5 Hz, ph-C_2 and C_6-H), 8.42 (d, 2H, J = 9 Hz, ph-C_3 and C_5-H); ^{13}C NMR (400 MHz, $CDCl_3$) δ ppm: 12.97 (2CH_3), 110.12 (pyrrole-C_3 and C_4), 127.59 (pyrrole-C_2 and C_5), 129.03 (ph-C_2 and C_6), 131.06 (ph-C_3 and C_5), 132.87 (ph-C_1), 137.57 (ph-C_4), 161.13 (thiadiazole-C_2), 164.25 (thiadiazole-C_5); MS (EI): m/z = found 300.23 [M^+], 301.23 [M^++1]; calcd. 300.07. Anal. $C_{14}H_{12}N_4O_2S$.

2-(4-Bromophenyl)-5-(2,5-dimethyl-1*H*-pyrrol-1-yl)-1,3,4-thiadiazole (5e)

Yield, 44%: mp 108°C–110°C; FTIR (KBr): 2,917 and 2,854 (Ar-H), 1,585 (C=N) cm^{-1}; ^{1}H NMR (400 MHz, DMSO-d_6) δ ppm: 2.25 (s, 6H, 2CH_3), 5.94 (s, 2H, pyrrole-C_3 and C_4-H), 7.95 (d, 2H, J = 5.35 Hz, ph-C_3 and C_5-H), 8.07 (d, 2H, J = 5.33 Hz, ph-C_2 and C_6-H); ^{13}C NMR (400 MHz, DMSO-d_6) δ ppm: 13.01 (2CH_3), 109.03 (pyrrole-C_3 and C_4), 129.22 (pyrrole-C_2 and C_5), 129.30 (ph-C_2 and C_6), 130.05 (ph-C_3 and C_5), 133.26 (ph-C_1), 138.54 (ph-C_4), 160.23 (thiadiazole-C_2), 165.15 (thiadiazole-C_5); MS (EI): m/z = found 332.56 [M^+], 334.56 [M^+ +2]; calcd. 332.99. Anal. $C_{14}H_{12}BrN_3S$.

2-(4-Methylphenyl)-5-(2,5-dimethyl-1*H*-pyrrol-1-yl)-1,3,4-thiadiazole (5f)

Yield, 53%: mp 92°C–94°C; FTIR (KBr): 2,921 and 2,857 (Ar-H), 1,603 (C=N) cm^{-1}; ^{1}H NMR (400 MHz, $CDCl_3$) δ ppm: 2.24 (s, 6H, 2CH_3), 2.42 (s, 3H, CH_3), 5.93 (s, 2H, pyrrole-C_3 and C_4-H), 7.37 (d, 2H, J = 5.05 ph-C_3 and C_5-H), 7.88 (d, 2H, J = 5.10 ph-C_2 and C_6-H); ^{13}C NMR (400 MHz, $CDCl_3$) δ ppm: 13.33 (2CH_3), 25.02 (CH_3), 110.06 (pyrrole-C_3 and C_4), 128.59 (pyrrole-C_2 and C_5), 129.17 (ph-C_2 and C_6), 131.00 (ph-C_3 and C_5), 133.22 (ph-C_1), 136.52 (ph-C_4), 159.69 (thiadiazole-C_2), 163.29 (thiadiazole-C_5); MS (EI): m/z =found 269.03 [M^+]; calcd. 269.10. Anal. $C_{15}H_{15}N_3S$.

2-(4-Aminophenyl)-2-(2,5-dimethyl-1*H*-pyrrol-1-yl)-1,3,4-thiadiazole (5g)

Yield, 21%: mp 196°C–198°C; FTIR (KBr): 3,244 (NH_2), 2,922 and 2,853 (Ar-H), 1,652 (C=N) cm^{-1}; ^{1}H NMR (400 MHz, $CDCl_3$) δ ppm: 2.06 (s, 6H, 2CH_3), 5.85 (s, 2H, pyrrole-C_3 and C_4-H), 7.38 (s, 2H, NH_2), 7.98–8.15 (m, 4H, ph-C_2, C_3, C_5 and C_6-H); ^{13}C NMR (400 MHz, $CDCl_3$) δ ppm: 13.22 (2CH_3), 108.69 (pyrrole-C_3 and C_4), 127.53 (pyrrole-C_2 and C_5), 129.36 (ph-C_2 and C_6), 130.59 (ph-C_3 and C_5), 132.05 (ph-C_1), 138.42 (ph-C_4), 161.00 (thiadiazole-C_2), 164.67 (thiadiazole-C_5); MS (EI): m/z = found 270.17 [M^+]; calcd. 270.09. Anal. $C_{14}H_{14}N_4S$.

2-(4-Fluorophenyl)-5-(2,5-dimethyl-1*H*-pyrrol-1-yl)-1,3,4-thiadiazole (5h)

Yield, 41%: mp 118°C–120°C; FTIR (KBr): 2,920 and 2,852 (Ar-H), 1,612 (C=N) cm^{-1}; ^{1}H NMR (400 MHz, $CDCl_3$) δ ppm: 2.25 (s, 6H, 2CH_3), 5.94 (s, 2H, pyrrole-C_3 and C_4-H), 7.30–8.07 (m, 4H, ph-C_2, C_3, C_5 and C_6-H); ^{13}C NMR (400 MHz, $CDCl_3$) δ ppm: 12.97 (2CH_3), 105.83 (pyrrole-C_3 and C_4), 116.37 (ph-C_3 and C_5), 129.33 (pyrrole-C_2 and

C_5), 129.53 (ph-C_1, C_2 and C_6), 132.23 (ph-C_4), 159.88 (thiadiazole-C_2), 163.05 (thiadiazole-C_5); MS (EI): m/z = found 273.01 [M^+]; calcd. 273.07. Anal. $C_{14}H_{12}FN_3S$.

2-(2,5-Dimethyl-1*H*-pyrrol-1-yl)-5-(pyridin-3-yl)-1,3,4-thiadiazole (5i)

Yield, 39%: mp 103°C–105°C; FTIR (KBr): 2,918 and 2,855 (Ar-H), 1,602 (C=N) cm^{-1}; ^1H NMR (400 MHz, $CDCl_3$) δ ppm: 2.26 (s, 6H, $2CH_3$), 5.83 (s, 2H, pyrrole-C_3 and C_4-H), 7.42–8.77 (m, 4H, pyridine-C_2, C_4, C_5 and C_6-H); ^{13}C NMR (400 MHz, $CDCl_3$) δ ppm: 12.89 ($2CH_3$), 105.73 (pyrrole-C_3 and C_4), 123.16 (pyridine-C_5), 129.31 (pyrrole-C_2 and C_5), 131.24 (pyridine-C_3), 133.57 (pyridine-C_4), 148.03 (pyridine-C_6), 148.99 (pyridine-C_2), 163.22 (thiadiazole-C_2), 174.03 (thiadiazole-C_5); MS (EI): m/z = found 256.13 [M^+]; calcd. 256.08. Anal. $C_{13}H_{12}N_4S$.

Synthesis of 2-(1*H*-pyrrol-1-yl)-5-sulfonamido-1,3,4-thiadiazole (8a)

To a solution of 2-amino-5-sulfonamido-1,3,4-thiadiazole (10 mmol) in 20 mL glacial acetic acid, 2,5-dimethoxytetrahydrofuran (15 mmol) was added slowly at room temperature and was refluxed for 1 hour (monitored by TLC). The reaction mixture was poured into ice-cold water and basified with sodium bicarbonate solution. The separated solid was collected, washed with water, dried, and recrystallized from aqueous ethanol.

Yield, 40%: mp 188°C–190°C; FTIR (KBr): 3,358.53, 3,253.98 (SO_2NH_2), 3,108.56 (Ar-H), 1,514.81 (C=N), 1,347.45 (SO_2^{as}), 1,174.42 (SO_2^{sym}) cm^{-1}; ^1H NMR (400 MHz, $CDCl_3$) δ ppm: 6.46 (s, 2H, pyrrole-C_3 and C_4-H), 7.61 (s, 2H, pyrrole-C_2, C_5-H), 8.59 (s, 2H, NH_2); ^{13}C NMR (400 MHz, $CDCl_3$) δ ppm: 114.21 (pyrrole-C_3 and C_4), 122.13 (pyrrole-C_2 and C_5), 165.29 (thiadiazole-C_2), 166.32 (thiadiazole-C_5); MS (EI): m/z = found 229.07 [M^+]; calcd. 229.99. Anal. $C_6H_6N_4O_2S_2$.

Synthesis of 2-(2,5-dimethyl-1*H*-pyrrol-1-yl)-5-sulfonamido-1,3,4-thiadiazole (8b)

To a solution of 2-amino-5-sulfonamido-1,3,4-thiadiazole (10 mmol) in 20 mL glacial acetic acid, acetonyl acetone (15 mmol) was added slowly at room temperature and was refluxed for 30 minutes. The reaction mixture was poured into ice-cold water and basified with sodium bicarbonate solution. The separated solid was collected, washed with water, dried, and recrystallized from ethanol.

Yield, 30%: mp 206°C–208°C; FTIR (KBr): 3,274.75, 3,085.68 (SO_2NH_2), 2,773.97 (Ar-H), 1,513.63 (C=N) 1,316.14 (SO_2^{as}), 1,129.71 (SO_2^{sym}) cm^{-1}; ^1H NMR (400 MHz, $CDCl_3$) δ ppm: 1.80 (s, 6H, pyrrole-$2CH_3$), 5.60 (s, 2H, pyrrole-C_3 and C_4-H), 8.52 (s, 2H, NH_2); ^{13}C NMR (400 MHz, $CDCl_3$) δ ppm: 12.81 ($2CH_3$), 115.23 (pyrrole-C_3 and C_4), 121.98 (pyrrole-C_2 and C_5), 164.88 (thiadiazole-C_2), 166.03 (thiadiazole-C_5); MS (EI): m/z = found 258.19 [M^+]; calcd. 258.02. Anal. $C_8H_{10}N_4O_2S_2$.

Biological evaluation

Antitubercular activity

The MIC values were determined for the newly synthesized compounds (4a–4i, 5a–5i, and 8a–8b) against *M. tuberculosis* strain $H_{37}Rv$, using a microplate Alamar blue assay.[33] Isoniazid was used as the standard drug. The 96-well plate received 100 µL of the Middlebrook 7H9 broth, and serial dilution of compounds was made directly on the plate. The final drug concentrations tested were 0.2, 0.4, 0.8, 1.6, 3.125, 6.25, 12.5, 25, 50, and 100 µg mL^{-1}. Plates were covered and sealed with parafilm and incubated at 37°C for 5 days. After this, 25 µL freshly prepared 1:1 mixture of Alamar blue reagent and 10% Tween 80 was added to the plate and incubated for 24 hours. A blue color in the well was interpreted as no bacterial growth, and a pink color was scored as the growth. The MIC was defined as the lowest drug concentration that prevented the color change from blue to pink. Table 1 reveals the antitubercular activity (MIC) data of the newly synthesized compounds.

Molecular modeling

General procedure

The 3D structure building and all modeling protocols were performed using the Sybyl-X 2.0 programming package running on a dual-core Intel core i3-2130 CPU 3.40 GHz, RAM Memory 2 GB workstation running Windows 7. Each structure was geometrically optimized using a conjugate gradient method based on Tripos force field[34] and MMFF94 charge, with a distance-dependant dielectric and Powell conjugate gradient algorithm with a convergence criterion of 0.01 kcal/mol. Partial atomic charges were calculated using the semiempirical program MOPAC 6.0, as well as by applying the AM1 Hamiltonian (Austin Model 1).[35]

Protein preparation

Crystal structure of *M. tuberculosis* enoyl reductase (InhA) complexed with 1-cyclohexyl-*N*-(3,5-dichlorophenyl)-5-oxopyrrolidine-3-carboxamide was retrieved from Research Collaboratory for Structural Bioinformatics Protein Data Bank (PDB ID code 4TZK).[12] Water molecules were removed, and essential hydrogens were added; united atoms

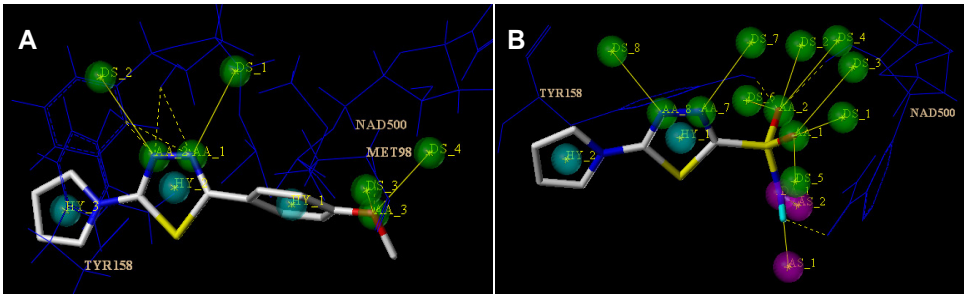

Figure 14 Pharmacophoric and receptor binding features (cyan, hydrophobic; green, H-bond acceptor; magenta, H-bond donor) for compounds 4b (**A**) and 8a (**B**) (capped sticks model in atom type color).

Amber7FF9902 were assigned for the protein. Geometry optimization was carried out using the standard Tripos force field, with a distance-dependent dielectric function keeping the energy gradient of 0.001 kcal/mol. Surflex-Dock is one of the best docking suites employed for docking analysis.[36,37]

Conclusion

Most of the synthesized compounds exhibited moderate activity against *M. tuberculosis.* Compounds 4b, 5b, and 5d inhibited growth of *M. tuberculosis* very effectively at a MIC value of 12.5 µg/mL, followed by compounds 4d, 4h, 4i, 5h, 5i, 8a, and 8b, with MIC values 25 µg/mL. Most of the molecules could effectively bind to the substrate binding site of ENR. The key H-bonding interactions with Tyr158, Met98, and cofactor NAD^+, as well as hydrophobic amino acid residues, stabilized the ligand–receptor complex to conclude that molecules are efficiently bound at the active site of ENR and, hence, can be better ENR inhibitors. To accomplish the inhibitory action, H-bond acceptor atoms and hydrophobic fragments played a key role (Figure 14). The predicted in silico Surflex-Dock values obtained through docking studies have pointed toward 4b, 5d, and 8a as the most promising inhibitors. Conclusively, compounds substituted with $-OCH_3$, $-NO_2$, -F, pyridine, and sulfonamide groups or moieties were found to be better inhibitors than compounds substituted with $-CH_3$, $-NH_2$, -Cl, and -Br groups. All the synthesized compounds showed a reasonable correlation between the experimental and predicted results. The present study suggests that molecular docking and in vitro MIC assay analysis could serve to be an efficient prescreening technique for identifying new ENR inhibitors and may be useful in situations in which enzyme inhibition experimental data are insufficient or not available.

Acknowledgments

We thank the Indian Council of Medical Research, New Delhi, India, for financial support (File 64/4/2011-BMS, IRIS Cell 2010-08710) and acknowledge partial financial support from the Vision Group on Science and Technology, Department of Information Technology, Biotechnology and Science and Technology, Dr S Ananth Raj, Bangalore (File VGST/P-3/SMYSR/GRD-277/2013-14/, dated January 28, 2014). We also thank Mr HV Dambal, president and Dr VH Kulkarni, principal, Soniya Education Trust's College of Pharmacy, Dharwad, India, for providing facilities. We thank Dr KG Bhat, Maratha Mandal's Dental College, Hospital and Research Centre, Belgaum, India, for providing facilities for antitubercular activity. The director, Sophisticated Analytical Instrument Facility (SAIF), Indian Institute of Technology, Chennai, Tamil Nadu, India, and the director, SAIF, Panjab University, Chandigarh, Panjab, India, have provided NMR and mass spectral data. We also thank Mr Shrikant A Tiwari for his technical assistance.

Disclosure

The authors report no conflicts of interest in this work.

References

1. Bogatcheva E, Hanrahan C, Nikonenko B, et al. Identification of new diamine scaffolds with activity against *Mycobacterium tuberculosis. J Med Chem*. 2006;49(11):3045–3048.
2. Rattan A, Kalia A, Ahmad N. Multidrug-resistant *Mycobacterium tuberculosis*: molecular perspectives. *Emerg Infect Dis*. 1998;4(2): 195–209.
3. Bloch K. Control mechanisms for fatty acid synthesis in *Mycobacterium smegmatis. Adv Enzymol Relat Areas Mol Biol*. 1977;45:1–84.
4. Kikuchi S, Rainwater DL, Kolattukudy PE. Purification and characterization of an unusually large fatty acid synthase from *Mycobacterium tuberculosis* var. bovis BCG. *Arch. Biochem Biophys*. 1992;295(2): 318–326.
5. Qureshi N, Sathyamoorthy N, Takayama K. Biosynthesis of C30 to C56 fatty acids by an extract of *Mycobacterium tuberculosis* H37Ra. *J Bacteriol*. 1984;157(1):46–52.
6. Brennan PJ, Nikaido H. The envelope of mycobacteria. *Annu Rev Biochem*. 1995;64(1):29–63.
7. Lee RE, Brennan PJ, Besra GS. *Mycobacterium tuberculosis* cell envelope. *Curr Top Microbiol Immunol*. 1996;215:1–27.
8. Banerjee A, Dubnau E, Quemard A, et al. inhA, a gene encoding a target for isoniazid and ethionamide in *Mycobacterium tuberculosis. Science*. 1994;263(5144):227–230.

9. Wang F, Langley R, Gulten G, et al. Mechanism of thioamide drug action against tuberculosis and leprosy. *J Exp Med*. 2007;204(1):73–78.
10. Kuo MR, Morbidoni HR, Alland D, et al. Targeting tuberculosis and malaria through inhibition of Enoyl reductase: compound activity and structural data. *J Biol Chem*. 2003;278(23):20851–20859.
11. Sullivan TJ, Truglio JJ, Boyne ME, et al. High affinity InhA inhibitors with activity against drug-resistant strains of *Mycobacterium tuberculosis. ACS Chem Biol*. 2006;1(1):43–53.
12. He X, Alian A, Stroud R, Ortiz de Montellano PR. Pyrrolidine carboxamides as a novel class of inhibitors of enoyl acyl carrier protein reductase from *Mycobacterium tuberculosis. J Med Chem*. 2006;49(21): 6308–6323.
13. Joshi SD, More UA, Kulkarni VH, Aminabhavi TM. Pyrrole: chemical synthesis, microwave assisted synthesis, reactions and applications: A review. *Curr Org Chem*. 2013;17(20):2279–2304.
14. Bhat AR, Tazeem, Azam A, Choi I, Athar F. 3-(1,3,4-Thiadiazole-2-yl) quinoline derivatives: synthesis, characterization and anti-microbial activity. *Eur J Med Chem*. 2011;46(7):3158–3166.
15. Talath S, Gadad AK. Synthesis, antibacterial and antitubercular activities of some 7-[4-(5-amino-[1,3,4]thiadiazole-2-sulfonyl)-piperazin-1-yl] fluoroquinolonic derivatives. *Eur J Med Chem*. 2006;41(8):918–924.
16. Foroumadi A, Kargar Z, Sakhteman A, et al. Synthesis and antimycobacterial activity of some alkyl [5-(nitroaryl)-1,3,4-thiadiazol-2-ylthio] propionates. *Bioorg Med Chem Lett*. 2006;16(5):1164–1167.
17. More UA, Joshi SD, Aminabhavi TM, Gadad AK, Nadagouda MN, Kulkarni VH. Design, synthesis, molecular docking and 3D-QSAR studies of potent inhibitors of enoyl-acyl carrier protein reductase as potential antimycobacterial agents. *Eur J Med Chem*. 2014;71:199–218.
18. More UA, Joshi SD, Kulkarni VH. Antitubercular activity of pyrrole Schiff bases and computational study of *M. tuberculosis* InhA. *Int J Drug Design Disc.* 2013;4:1163–1173.
19. Joshi SD, More UA, Aminabhavi TM, Badiger AM. Two- and three-dimensional QSAR studies on a set of antimycobacterial pyrroles: CoMFA, Topomer CoMFA, and HQSAR. *Med Chem Res*. 2014;23(1): 107–126.
20. Joshi SD, More UA, Dixit SR, Korat HH, Aminabhavi TM, Badiger AM. Synthesis, characterization, biological activity, and 3D-QSAR studies on some novel class of pyrrole derivatives as antitubercular agents. *Med Chem Res*. 2014;23(3):1123–1147.
21. Joshi SD, Dixit SR, More UA, Devendra K, Aminabhavi TM, Kulkarni VH. 3D-QSAR studies of quinoline Schiff bases as enoyl acyl carrier protein reductase inhibitors. *Res Rep Med Chem*. 2014;4:59–75.
22. Bukhari SN, Franzblau SG, Jantan I, Jasamai M. Current prospects of synthetic curcumin analogs and chalcone derivatives against *Mycobacterium tuberculosis. Med Chem*. 2013;9(7):897–903.
23. Joshi SD, Joshi A, Vagdevi HM, Vaidya VP, Gadaginamath GS. Synthesis and antimicrobial evaluation of some new pyrrolylnaphtho[2,1-*b*] furan derivatives. *Indian J Pharm Educ Res.* 2010;44:148–155.
24. Joshi SD, Joshi A, Vagdevi HM, Vaidya VP, Gadaginamath GS. Microwave assisted synthesis of some new quinolinylpyrrole derivatives as potential antibacterial and antitubercular agents. *Indian J Heterocycl Chem*. 2010;19:221–224.
25. Joshi SD, More Y, Vagdevi HM, Vaidya VP, Gadaginamath GS, Kulkarni VH. Synthesis of new 4-(2,5-dimethylpyrrol-1-yl)/4-pyrrol-1-yl benzoic acid hydrazide analogs and some derived oxadiazole, triazole and pyrrole ring systems a novel class of potential antibacterial, antifungal and antitubercular agents. *Med Chem Res*. 2013;22(3):1073–1089.
26. Joshi SD, Manish K, Badiger A. Synthesis and evaluation of antibacterial and antitubercular activities of some novel imidazo[2,1-*b*][1,3,4] thiadiazole derivatives. *Med Chem Res*. 2013;22(2):869–878.
27. Joshi SD, Vagdevi HM, Vaidya VP, Gadaginamath GS. Synthesis of new 4-pyrrol-1-yl benzoic acid hydrazide analogs and some derived oxadiazole, triazole and pyrrole ring systems,: a novel class of potential antibacterial and antitubercular agents. *Eur J Med Chem*. 2008;43(9): 1989–1996.
28. Kitchen DB, Decornez H, Furr JR, Bajorath J. Docking and scoring in virtual screening for drug discovery: methods and applications. *Nat Rev Drug Discov*. 2004;3(11):935–949.
29. Ho CM, Marshall GR. Cavity search: an algorithm for the isolation and display of cavity-like binding regions. *J Comput Aided Mol Des*. 1990;4(4):337–354.
30. Jain AN. Scoring noncovalent protein-ligand interactions: a continuous differentiable function tuned to compute binding affinities. *J Comput Aided Mol Des*. 1996;10(5):427–440.
31. Jain AN. Surflex: fully automatic flexible molecular docking using a molecular similarity-based search engine. *J Med Chem*. 2003;46(4): 499–511.
32. Tu G, Li S, Huang H, et al. Novel aminopeptidase N inhibitors derived from 1,3,4-thiadiazole scaffold. *Bioorg Med Chem*. 2008;16(14): 6663–6668.
33. Franzblau SG, Witzig RS, McLaughlin JC, et al. Rapid, low-technology MIC determination with clinical *Mycobacterium tuberculosis* isolates by using the microplate Alamar Blue assay. *J Clin Microbiol*. 1998;36(2): 362–366.
34. Clark M, Cramer RD III, Opdenbosch NV. Validation of the general purpose tripos 5.2 forcefield. J Comput Chem. 1989;10(8):982–1012.
35. Stewart JJ. ; StewartJJ. MOPAC: a semiempirical molecular orbital program. *J* Comput Aided Mol Des. 1990;4(1):1–105.
36. Spitzer R, Jain AN. Surflex-Dock: docking benchmarks and real-world application. *J Comput Aided Mol Des*. 2012;26(6):687–699.
37. Pham TA, Jain AN. Customizing scoring functions for docking. *J Comput Aided Mol Des*. 2008;22(5):269–286.

Supplementary materials

Pharmacophore mapping

During the study, it was found that the InhA inhibitor [1-cyclohexyl-*N*-(3,5-dichlorophenyl)-5-oxopyrrolidine-3-carboxamide (pyrrolidine carboxamide or 641)], which contains three hydrophobic moieties, such as cyclohexyl, oxopyrrolidine, and 3,5-dichlorophenyl, can be replaced by new, designed molecules, which contain pyrrole, 1,3,4-thiadiazole, and substituted phenyl. Hydrogen bond acceptor atoms such as oxygen at the fifth position of pyrrolidine and nitrogens at 1,3,4-thiadiazole make an H-bond with key amino acid Tyr158 and cofactor NAD^+, which helps in structure-based drug design and the selection of target.

Hydropathy plots

In hydropathy, produce scatter plots of the hydropathy indices as a function of the residue number. Such plots are frequently used to identify segments of a protein sequence that have hydrophobic properties consistent with a transmembrane helix.

Three columns are added to the spreadsheet: HYDRO is the hydrophobicity at each residue, with its value depending on the hydrophobicity scale chosen. HYD_5 is the hydropathy index averaged over a moving window of eleven residues (five on either side of a given residue). The window size determines the extent of smoothing for the calculation of hydropathy indices. SEQNUM is an integer corresponding to the serial position of the residue in the protein. It is a useful index when residue numbering does not start at one or is not sequential.

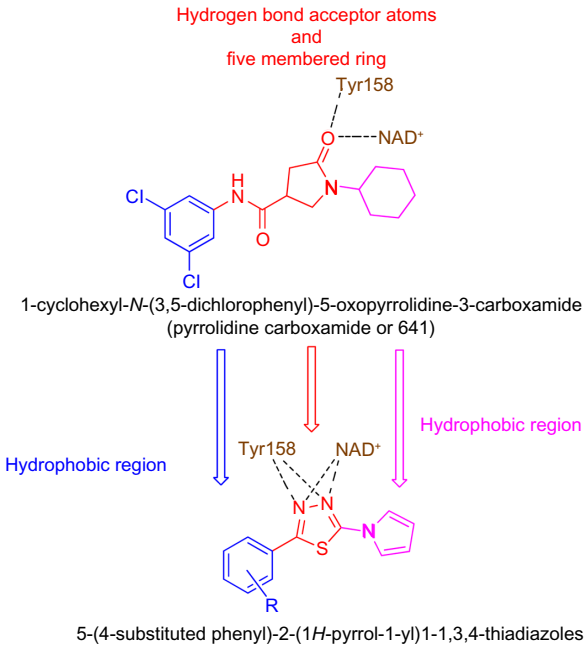

Figure S1 Structure-based drug design concept.

Table S1 Hydrophobicity scales for protein

Name	HYDRO	HYD_5	SEQNUM	Name	HYDRO	HYD_5	SEQNUM
AMN1	–	–	1	PRO136	−1.6	0.6	136
THR2	−0.7	–	2	ILE137	4.5	0.4	137
GLY3	−0.4	–	3	MET138	1.9	0.6818	138
LEU4	3.8	–	4	ASN139	−3.5	0.9273	139
LEU5	3.8	–	5	PRO140	−1.6	0.9636	140
ASP6	−3.5	0.2273	6	GLY141	−0.4	0.5818	141
GLY7	−0.4	0.6091	7	GLY142	−0.4	0.9	142
LYS8	−3.9	0.6	8	SER143	−0.8	0.1727	143
ARG9	−4.5	0.6	9	ILE144	4.5	0.2545	144
ILE10	4.5	0.6636	10	VAL145	4.2	0.2545	145
LEU11	3.8	0.7273	11	GLY146	−0.4	0.2545	146
VAL12	4.2	0.9818	12	MET147	1.9	0.2182	147
SER13	−0.8	0.7	13	ASP148	−3.5	−0.1545	148
GLY14	−0.4	0.9818	14	PHE149	2.8	0.0818	149
ILE15	4.5	1.3182	15	ASP150	−3.5	−0.1545	150
ILE16	4.5	1.3182	16	PRO151	−1.6	−0.6818	151
THR17	−0.7	1.1364	17	SER152	−0.8	−0.4818	152
ASP18	−3.5	1.0091	18	ARG153	−4.5	−0.7727	153
SER19	−0.8	0.7909	19	ALA154	1.8	−0.7727	154
SER20	−0.8	1.2364	20	MET155	1.9	−1.1091	155
ILE21	4.5	0.9909	21	PRO156	−1.6	−0.6182	156
ALA22	1.8	0.1727	22	ALA157	1.8	−0.5364	157
PHE23	2.8	0.6182	23	TYR158	−1.3	−0.0818	158
HIS24	−3.2	1.1	24	ASN159	−3.5	0.4909	159
ILE25	4.5	0.8545	25	TRP160	−0.9	−0.0273	160
ALA26	1.8	0.6091	26	MET161	1.9	−0.2727	161
ARG27	−4.5	−0.1182	27	THR162	−0.7	0.0364	162
VAL28	4.2	−0.3182	28	VAL163	4.2	0.2182	163
ALA29	1.8	−0.4091	29	ALA164	1.8	0.0182	164
GLN30	−3.5	−0.4364	30	LYS165	−3.9	0.2636	165
GLU31	−3.5	−0.5	31	SER166	−0.8	0.7273	166
GLN32	−3.5	−0.2818	32	ALA167	1.8	0.2364	167
GLY33	−0.4	0.4727	33	LEU168	3.8	−0.1091	168
ALA34	1.8	0.0273	34	GLU169	−3.5	−0.2364	169
GLN35	−3.5	−0.1727	35	SER170	−0.8	−0.0182	170
LEU36	3.8	0.4	36	VAL171	4.2	0.5	171
VAL37	4.2	0.4	37	ASN172	−3.5	0.1636	172
LEU38	3.8	0.3091	38	ARG173	−4.5	−0.3182	173
THR39	−0.7	0.6909	39	PHE174	2.8	−0.5	174
GLY40	−0.4	0.1182	40	VAL175	4.2	−0.2182	175
PHE41	2.8	0.7818	41	ALA176	1.8	−0.5	176
ASP42	−3.5	0.8455	42	ARG177	−4.5	−1	177
ARG43	−4.5	0.1455	43	GLU178	−3.5	−0.7182	178
LEU44	3.8	−0.6091	44	ALA179	1.8	0.0727	179
ARG45	−4.5	−0.1364	45	GLY180	−0.4	−0.5909	180
LEU46	3.8	−0.1636	46	LYS181	−3.9	−1.0455	181
ILE47	4.5	−0.7364	47	TYR182	−1.3	−1.5273	182
GLN48	−3.5	−0.8273	48	GLY183	−0.4	−0.7727	183
ARG49	−4.5	−0.0727	49	VAL184	4.2	−0.0727	184
ILE50	4.5	−0.5636	50	ARG185	−4.5	−0.0727	185
THR51	−0.7	0.0091	51	SER186	−0.8	0.1273	186
ASP52	−3.5	−0.6909	52	ASN187	−3.5	0.4455	187
ARG53	−4.5	−0.9364	53	LEU188	3.8	0.4182	188
LEU54	3.8	−0.7636	54	VAL189	4.2	0.8636	189

(*Continued*)

Table S1 (*Continued*)

Name	HYDRO	HYD_5	SEQNUM	Name	HYDRO	HYD_5	SEQNUM
PRO55	−1.6	−0.0091	55	ALA190	1.8	0.0727	190
ALA56	1.8	−0.0727	56	ALA191	1.8	0.4182	191
LYS57	−3.9	−0.3273	57	GLY192	−0.4	0.8364	192
ALA58	1.8	0.3364	58	PRO193	−1.6	1.3182	193
PRO59	−1.6	0.4273	59	ILE194	4.5	1.1455	194
LEU60	3.8	0.4636	60	ARG195	−4.5	0.6909	195
LEU61	3.8	0.2909	61	THR196	−0.7	0.6909	196
GLU62	−3.5	−0.1909	62	LEU197	3.8	0.9364	197
LEU63	3.8	−0.1545	63	ALA198	1.8	1.3545	198
ASP64	−3.5	−0.6364	64	MET199	1.9	1.4636	199
VAL65	4.2	−0.7818	65	SER200	−0.8	1.0182	200
GLN66	−3.5	−0.7818	66	ALA201	1.8	1.5909	201
ASN67	−3.5	−0.9636	67	ILE202	4.5	2	202
GLU68	−3.5	−0.7182	68	VAL203	4.2	1.6182	203
GLU69	−3.5	−0.7182	69	GLY204	−0.4	1.1364	204
HIS70	−3.2	−0.2364	70	GLY205	−0.4	0.6455	205
LEU71	3.8	−0.6545	71	ALA206	1.8	0.8818	206
ALA72	1.8	−0.7455	72	LEU207	3.8	0.6818	207
SER73	−0.8	−0.0455	73	GLY208	−0.4	0.4364	208
LEU74	3.8	0.2091	74	GLU209	−3.5	−0.2636	209
ALA75	1.8	0.2091	75	GLU210	−3.5	0.1818	210
GLY76	−0.4	0.6636	76	ALA211	1.8	−0.1	211
ARG77	−4.5	0.7273	77	GLY212	−0.4	0.0818	212
VAL78	4.2	0.5273	78	ALA213	1.8	0.0818	213
THR79	−0.7	0.7636	79	GLN214	−3.5	−0.2	214
GLU80	−3.5	0.3818	80	ILE215	4.5	−0.2	215
ALA81	1.8	−0.1	81	GLN216	−3.5	0.0818	216
ILE82	4.5	−0.4182	82	LEU217	3.8	−0.1636	217
GLY83	−0.4	0.3364	83	LEU218	3.8	−0.4455	218
ALA84	1.8	−0.3636	84	GLU219	−3.5	−0.9273	219
GLY85	−0.4	−0.3364	85	GLU220	−3.5	−1.0182	220
ASN86	−3.5	0.3636	86	GLY221	−0.4	−1.2636	221
LYS87	−3.9	0.5818	87	TRP222	−0.9	−1.0909	222
LEU88	3.8	−0.1182	88	ASP223	−3.5	−1.0273	223
ASP89	−3.5	−0.1545	89	GLN224	−3.5	−1.4091	224
GLY90	−0.4	0.0909	90	ARG225	−4.5	−1.1727	225
VAL91	4.2	0.0909	91	ALA226	1.8	−1.1727	226
VAL92	4.2	0.6636	92	PRO227	−1.6	−0.9636	227
HIS93	−3.2	1.1909	93	ILE228	4.5	−1.2364	228
SER94	−0.8	0.7	94	GLY229	−0.4	−1.2364	229
ILE95	4.5	0.7	95	TRP230	−0.9	−0.7545	230
GLY96	−0.4	0.6727	96	ASN231	−3.5	−0.4091	231
PHE97	2.8	0.2545	97	MET232	1.9	−0.7182	232
MET98	1.9	0.0455	98	LYS233	−3.9	−0.1909	233
PRO99	−1.6	0.3	99	ASP234	−3.5	−0.4364	234
GLN100	−3.5	0.7818	100	ALA235	1.8	−0.7545	235
THR101	−0.7	0.0545	101	THR236	−0.7	−0.7364	236
GLY102	−0.4	−0.0545	102	PRO237	−1.6	−0.0364	237
MET103	1.9	−0.0545	103	VAL238	4.2	0.0182	238
GLY104	−0.4	0.0273	104	ALA239	1.8	0.5364	239
ILE105	4.5	−0.1455	105	LYS240	−3.9	1.2	240
ASN106	−3.5	0.3364	106	THR241	−0.7	1.3818	241
PRO107	−1.6	0.2545	107	VAL242	4.2	1.3727	242
PHE108	2.8	0.1727	108	CYS243	2.5	1.2	243

(*Continued*)

Table S1 (*Continued*)

Name	HYDRO	HYD_5	SEQNUM	Name	HYDRO	HYD_5	SEQNUM
PHE109	2.8	0.1636	109	ALA244	1.8	0.7364	244
ASP110	−3.5	−0.1182	110	LEU245	3.8	0.9182	245
ALA111	1.8	−0.1455	111	LEU246	3.8	1.1273	246
PRO112	−1.6	0.1	112	SER247	−0.8	1.3545	247
TYR113	−1.3	−0.1091	113	ASP248	−3.5	0.9091	248
ALA114	1.8	−0.4	114	TRP249	−0.9	0.6182	249
ASP115	−3.5	−0.2455	115	LEU250	3.8	0.4182	250
VAL116	4.2	−0.2182	116	PRO251	−1.6	−0.2455	251
SER117	−0.8	0.0273	117	ALA252	1.8	−0.1818	252
LYS118	−3.9	0.1	118	THR253	−0.7	0.3	253
GLY119	−0.4	0.3818	119	THR254	−0.7	0.5	254
ILE120	4.5	0.1	120	GLY255	−0.4	0.7455	255
HIS121	−3.2	0.3455	121	ASP256	−3.5	0.0818	256
ILE122	4.5	−0.1545	122	ILE257	4.5	0.1909	257
SER123	−0.8	0.0818	123	ILE258	4.5	−0.0091	258
ALA124	1.8	0.3636	124	TYR259	−1.3	0.2182	259
TYR125	−1.3	0.5727	125	ALA260	1.8	−0.0091	260
SER126	−0.8	0.3273	126	ASP261	−3.5	−0.0364	261
TYR127	−1.3	0.2636	127	GLY262	−0.4	−0.0364	262
ALA128	1.8	0.0182	128	GLY263	−0.4	−0.1	263
SER129	−0.8	0.4364	129	ALA264	1.8	−0.1636	264
MET130	1.9	0.6182	130	HIS265	−3.2	−0.0455	265
ALA131	1.8	0.5909	131	THR266	−0.7	–	266
LYS132	−3.9	1.0727	132	GLN267	−3.5	–	267
ALA133	1.8	1.3636	133	LEU268	3.8	–	268
LEU134	3.8	0.8818	134	LEU269	3.8	–	269
LEU135	3.8	0.8091	135	CXL270	–	–	270

Notes: HYDRO, hydrophobicity at each residue, with value depending on the hydrophobicity scale chosen; HYD_5, the hydropathy index averaged over a moving window of eleven residues (five on either side of a given residue), and is the window size that determines the extent of smoothing for the calculation of hydropathy indices; SEQNUM, an integer corresponding to the serial position of the residue in the protein. It is a useful index when residue numbering does not start at one or is not sequential.